MICROCOPY RESOLUTION TEST CHART

NATIONAL BUREAU OF STANDARDS-1963-A

NAVAL POSTGRADUATE SCHOOL
Monterey, California

DTIC
S ELECTE D
DEC 1 5 1987
D

THESIS

A SURVEY OF SHIPBOARD COMBAT SURVIVABLE
VHF/UHF ANTENNAS

by

Henry Kevin Purvis

September 1987

Thesis Advisor   Richard W. Adler

87 12 9 147

NAVAL POSTGRADUATE SCHOOL

Monterey, CA 93943-5000

Rear Admiral R. C. Austin
Superintendent

K. T. Marshall
Acting Provost

This thesis prepared in conjunction with research sponsored
in part by Naval Ocean Systems Center.

Reproduction of all or part of this report is authorized.

Released by:

GORDON E. SCHACHER
Dean of Science and Engineering

AD A186 852

REPORT DOCUMENTATION PAGE

1a REPORT SECURITY CLASSIFICATION	1b RESTRICTIVE MARKINGS
UNCLASSIFIED	

2a SECURITY CLASSIFICATION AUTHORITY	3 DISTRIBUTION/AVAILABILITY OF REPORT
	Approved for public release distribution is unlimited
2b DECLASSIFICATION/DOWNGRADING SCHEDULE	

4 PERFORMING ORGANIZATION REPORT NUMBER(S)	5 MONITORING ORGANIZATION REPORT NUMBER(S)
- NPS-62-87-017	

6a NAME OF PERFORMING ORGANIZATION	6b OFFICE SYMBOL (If applicable)	7a NAME OF MONITORING ORGANIZATION
Naval Postgraduate School	62	Naval Ocean Systems Center

6c ADDRESS (City, State, and ZIP Code)	7b ADDRESS (City, State, and ZIP Code)
Monterey, California 93943-5100	SanDiego, California 92152

8a NAME OF FUNDING/SPONSORING ORGANIZATION	8b OFFICE SYMBOL (If applicable)	9 PROCUREMENT INSTRUMENT IDENTIFICATION NUMBER
Naval Ocean Systems Cntr	Code 825	N660186WR00516

8c ADDRESS (City, State, and ZIP Code)	10 SOURCE OF FUNDING NUMBERS			
	PROGRAM ELEMENT NO	PROJECT NO	TASK NO	WORK UNIT ACCESSION NO
San Diego, California 92152	62121N			

11 TITLE (Include Security Classification)

A Survey of Shipboard Combat Survivable VHF/UHF Antennas

12 PERSONAL AUTHOR(S)
Purvis, Henry K.

13a TYPE OF REPORT	13b TIME COVERED	14 DATE OF REPORT (Year, Month, Day)	15 PAGE COUNT
Master's Thesis	FROM ____ TO ____	1987 September	67

16 SUPPLEMENTARY NOTATION

17	COSATI CODES		18 SUBJECT TERMS (Continue on reverse if necessary and identify by block number)
FIELD	GROUP	SUB-GROUP	Combat Survivable Antennas, VHF/UHF; Computer Modeling of Antennas

19 ABSTRACT (Continue on reverse if necessary and identify by block number)

Antennas on modern ships protrude from the structure and are quite vulnerable to combat damage or inclement weather. Conformal antennas are needed to allow a ship to communicate after sustaining battle damage or heavy weather.

This thesis investigates three conformal antennas: a microstrip, a slot, and a combination monopole and slot. The principle of operation for each is discussed along with computer model results obtained from the Numerical Electromagnetics Code-Method of Moments and Basic Scattering Code.

20 DISTRIBUTION/AVAILABILITY OF ABSTRACT	21 ABSTRACT SECURITY CLASSIFICATION
☐ UNCLASSIFIED/UNLIMITED ☑ SAME AS RPT ☐ DTIC USERS	UNCLASSIFIED

22a NAME OF RESPONSIBLE INDIVIDUAL	22b TELEPHONE (Include Area Code)	22c OFFICE SYMBOL
Prof Richard W. Adler	(408) 646-2352	62Ab

DD FORM 1473, 84 MAR 83 APR edition may be used until exhausted

All other editions are obsolete

A Survey of Shipboard
Combat Survivable
VHF/UHF Antennas

by

Henry Kevin Purvis
Lieutenant, United States Navy
B-EET, Southern Technical Institute, 1979

Submitted in partial fulfillment of the
requirements for the degree of

MASTER OF SCIENCE IN ELECTRICAL ENGINEERING

from the

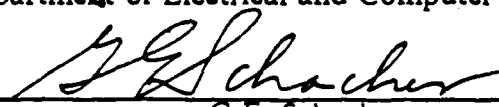NAVAL POSTGRADUATE SCHOOL
September 1987

Author: _____
Henry Kevin Purvis

Approved by: _____
R.W. Adler, Thesis Advisor

_____
H.A. Atwater, Second Reader

_____
J.P. Powers, Chairman,
Department of Electrical and Computer Engineering

_____
G.E. Schacher,
Dean of Science and Engineering

2

ABSTRACT

Antennas on modern ships protrude from the structure and are quite vulnerable to combat damage or inclement weather. Conformal antennas are needed to allow a ship to communicate after sustaining battle damage or heavy weather.

This thesis investigates three conformal antennas: a microstrip, a slot, and a combination monopole and slot. The principle of operation for each is discussed along with computer model results obtained from the Numerical Electromagnetics Code-Method of Moments and Basic Scattering Code.

Accesion For		
NTIS CRA&I	☑	
DTIC TAB	☐	
Unannounced	☐	
Justification		
By		
Distribution /		
Availability Codes		
Dist	Avail and/or Special	
A-1		

3

TABLE OF CONTENTS

5

LIST OF FIGURES

7

I. INTRODUCTION

A ship at sea that cannot communicate with the rest of the world is not only ineffective as a combat platform, but also extremely unsafe for its crew. Without communication channels with other units a ship cannot maintain a defense posture that would keep it afloat.

In order to preserve its communication ability, all elements of the communication system, from transmitter/receiver to antenna, must be able to survive combat damage as well as the inclement weather ships often face. While technology has been implemented to improve communication system performance, reduce size, provide redundancy, and protect elements inside the ship, antennas found on modern ships have not changed substantially in the past several years. They protrude from the ship's structure and are quite vulnerable to combat damage, high winds, or icing conditions. Future ship designs must be developed without the numerous fragile topside structures that make a ship vulnerable.

In the past several years, antennas have been developed that are quite efficient yet still electrically and physically small. Much work has been done on implementing antennas for airplanes and spacecraft that are low in profile. Studies are needed to extend the capabilities of these conformal antennas for shipboard use.

A. POSSIBLE UHF/VHF ANTENNAS FOR SHIPBOARD USE

Previous theses on this project have investigated exciting existing topside structures or slots in the side of a bulkhead for use as high frequency (HF) antennas. This could also be done for very high frequency (VHF) or ultra high frequency (UHF) antennas, but in these frequency ranges, the wavelength becomes small enough so that a microstrip or slot antenna would not be excessively large. This type of antenna could be mounted on a horizontal deck or vertical surface such as an exhaust stack.

Although microstrip and slotted antennas are conformal and produce acceptable radiation patterns, they do have serious drawbacks, one of the most serious being narrow bandwidth, commonly only a few percent. This would require a prohibitively large number of antennas for shipboard use.

The problem of narrow bandwidth has been addressed quite extensively in recent years. A few methods for widening the bandwidth of microstrip antennas are: using a

8

thicker substrate, using a ferrite substrate, using a wedge shaped substrate, adding stacked elements to a central element, adding additional directly coupled radiators, or adding additional gap coupled radiators. Some of these methods have been shown to improve the bandwidth from two or three percent up to and beyond twenty percent.

Methods for improving the bandwidth of slotted antennas include: multiple sized slots, changing the geometry of the slot (bowtie, wedge, etc), using inductively tuned posts, utilizing different feed methods (T-bar feed), placing ridges in a cavity backed slot, or utilizing the complementary nature of a slot and monopole.

The above methods were surveyed and three antennas were chosen for further investigation.

1. Microstrip Antenna Using Gap-Coupled Resonators

Although there are several methods that can be used for increasing the bandwidth of microstrip antennas, one method that has achieved considerable success without increasing the complexity of the antenna has been reported by Kumar and Gupta [Ref. 1: pp. 173-178]. This method consists of placing additional resonators in close proximity to a central micropatch element as shown in Figure 1.1 As shown, the additional radiators can be placed along two or four edges. The antenna input impedance can be controlled by varying the length of the additional resonators, the gap width, or feed point. Using two additional resonators, the bandwidth has been reported over three times that of a corresponding single element microstrip, while four resonators has been reported to deliver over six times the bandwidth of a single element.

2. Shallow Ridged-Cavity Crossed-Slot Antenna

The shallow ridged-cavity crossed-slot antenna, although developed for aircraft use, could be an excellent candidate for shipboard use. The antenna consists of a crossed slot backed by a shallow cavity containing nonuniformly shaped ridges as shown in Figure 1.2 This antenna exhibits hemispherical coverage over a wide range of frequencies (VSWR less than 3:1 from 240 MHz to 400 MHz) and circular polarization as reported by King and Wong. [Ref. 2: pp. 687-689]

3. Monopole-Slot Antenna

The monopole slot antenna shown in Figure 1.3 combines the complementary nature of slot antennas and monopole antennas to provide a relatively stable input resistance over a 10 to 1 bandwidth as reported by Mayes, Warren, and Weisenmeyer. [Ref. 3: pp. 489-493]

9
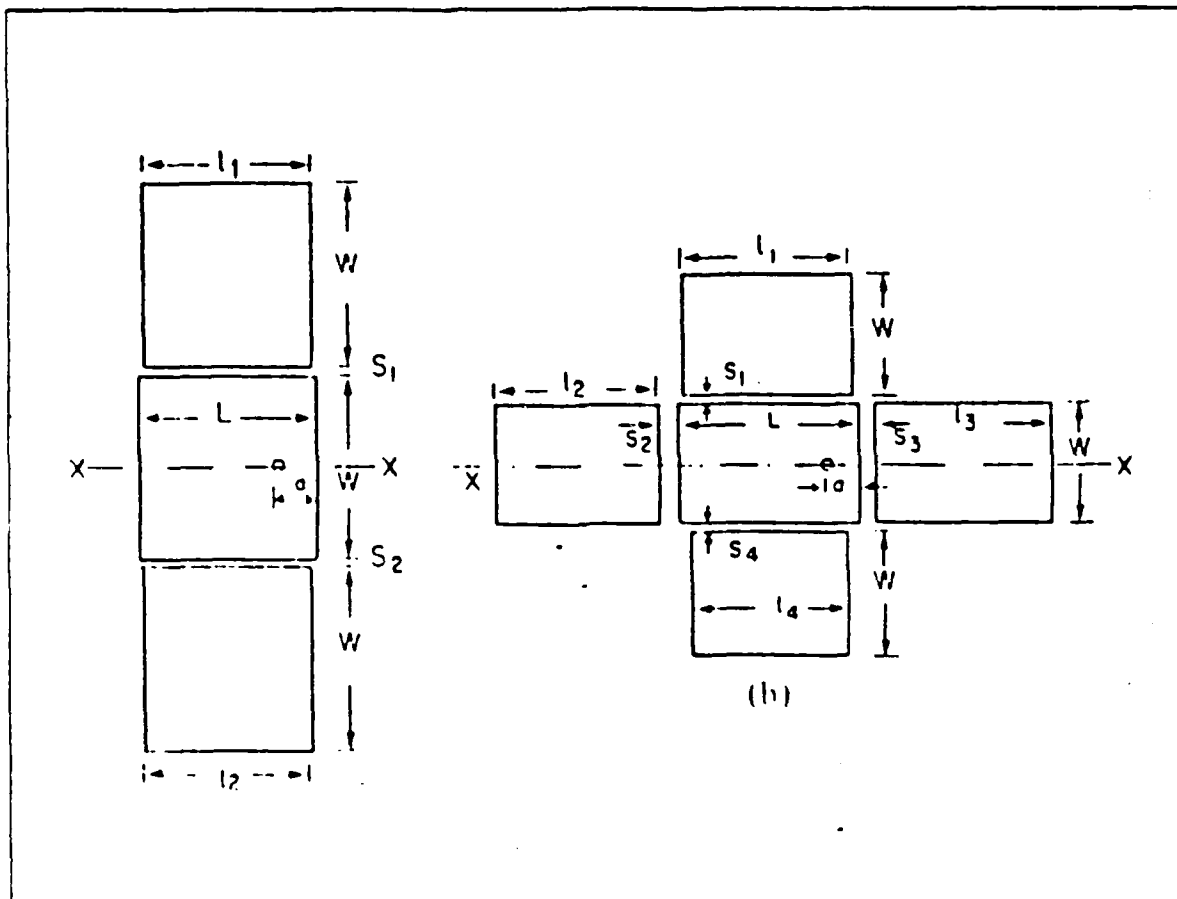
Figure 1.1 Gap-Coupled Multiple Resonator Microstrip Antennas
(from Ref. 1).

The monopole slot antenna consists of a slot backed by a shallow cavity and fed by a microstrip line. A short monopole antenna is placed on top of the microstrip at a position corresponding to the center of the slot. This configuration was later improved by top loading the monopole to reduce its height.

B. SCOPE OF WORK

This study is a survey of three conformal antennas which could be adapted for shipboard use. For the three antennas selected, each will be investigated as a first cut in determining their suitability as VHF/UHF communications antennas.

Chapter II will discuss the theory associated with simple halfwave microstrip antennas. Input impedance and radiation patterns will be discussed for later comparison with gap-coupled microstrip antennas. The gap-coupled microstrip antenna will be presented along with factors which affect the input impedance and
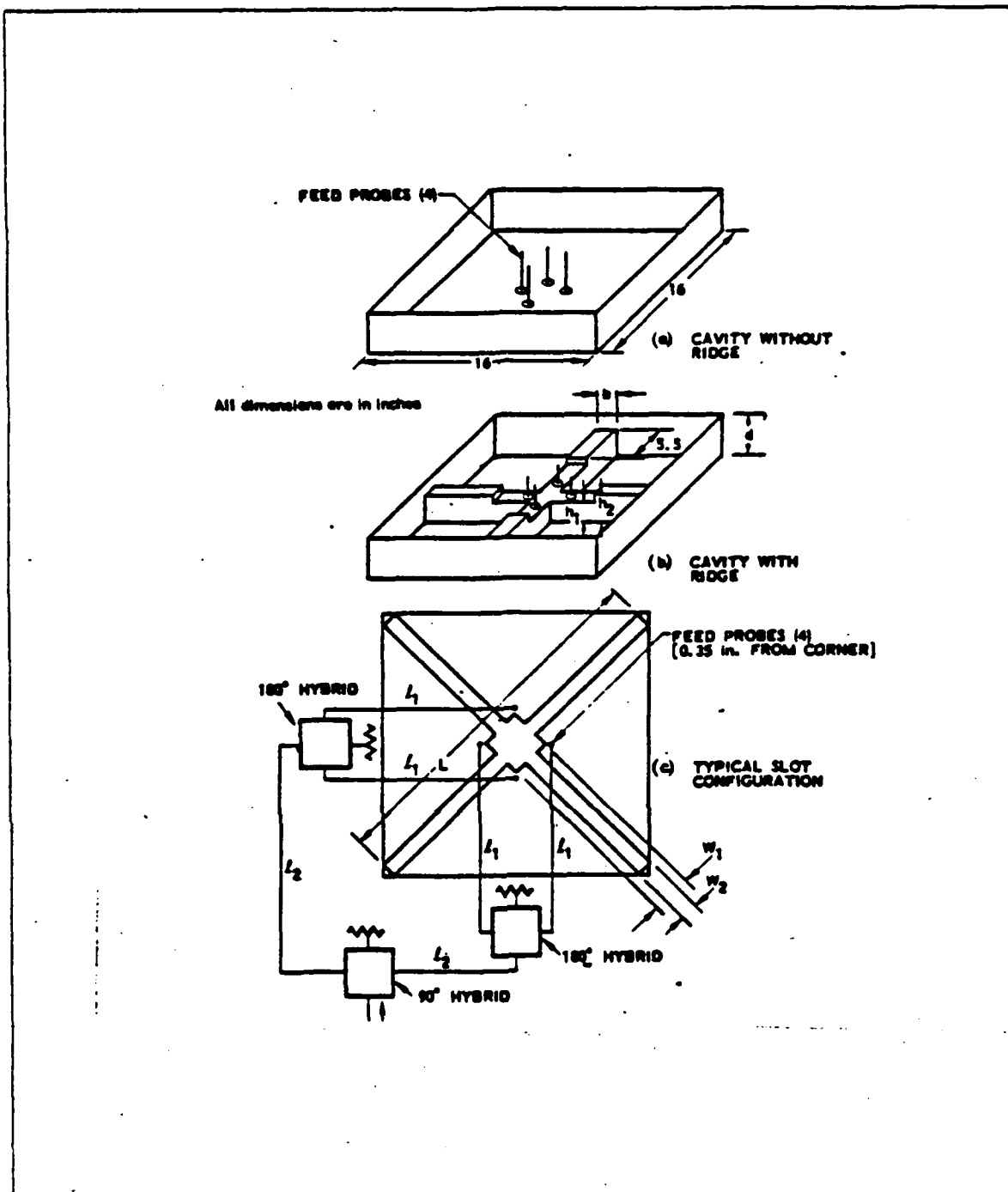
Figure 1.2   Ridged-Cavity Crossed-Slot Antenna (from Ref. 2).

radiation patterns. Chapter II will conclude with results of the computer model for a halfwave microstrip antenna and for the gap-coupled microstrip antenna. These antennas were modeled as wire grid patches using the Numerical Electromagnetics Code-Method of Moments (NEC-MOM) antenna modeling program.

11

NOTE: PORT 2 is terminated in 50-Ohms when S_{11} and S_{21} are measured.
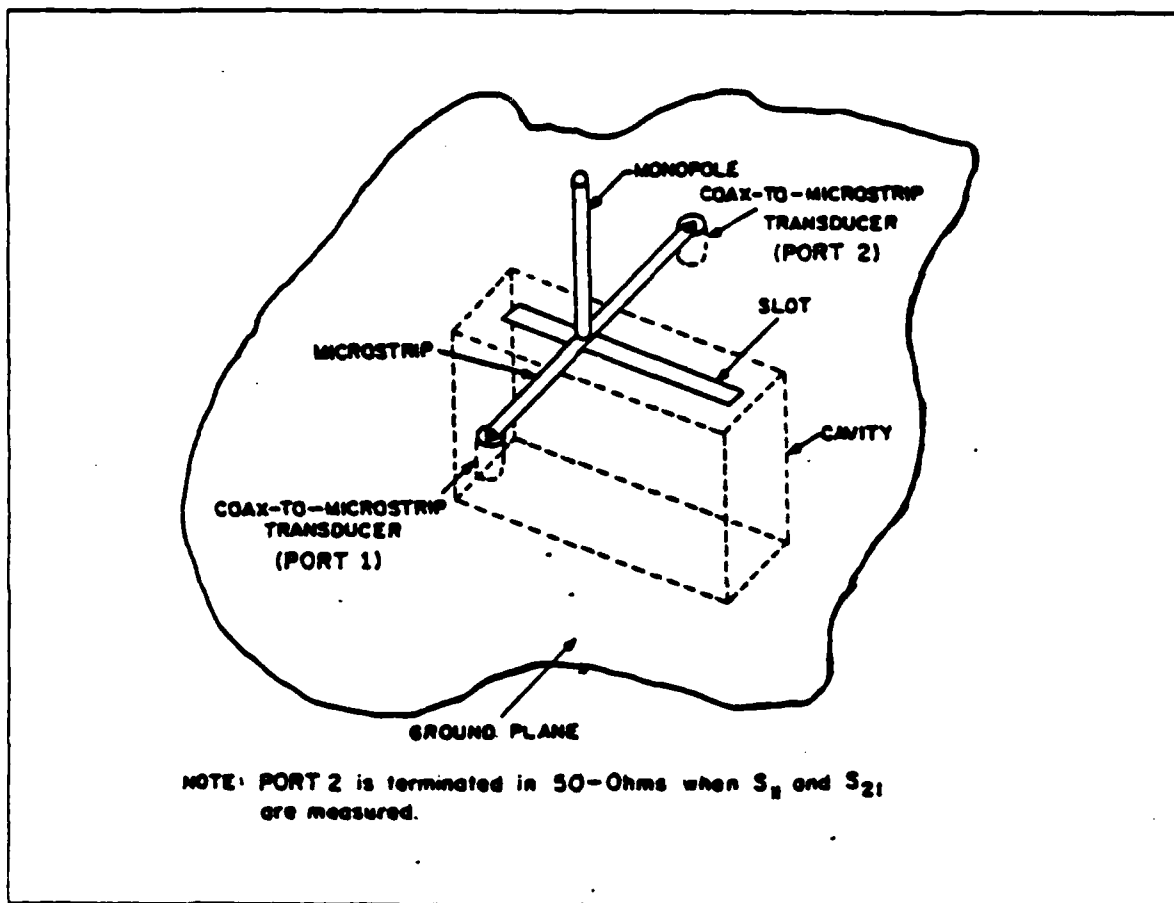
Figure 1.3 Stripline Fed Monopole-Slot Antenna (from Ref. 3).

Chapter III will discuss the ridged-cavity crossed-slot antenna and its operation. Although a computer model which duplicates this exact antenna is not presented, a simple crossed-slot antenna as modeled by the Numerical Electromagnetics Code-Basic Scattering Code (NEC-BSC) is given. This model is presented to show that a crossed-slot antenna can exhibit circular or elliptical polarization. The crossed-slot model will demonstrate the strong point of the NEC-BSC, that is, the ability to determine the radiation patterns of a simple antenna in a complex environment. Chapter III also includes an explanation of the NEC-BSC code, its principles and limitations.

Chapter IV includes a discussion of the monopole-slot antenna. The principle of operation for this antenna is discussed, while the principle of using complementary elements is demonstrated by the NEC-BSC.

12

II. MICROSTRIP ANTENNAS

A. HALF WAVELENGTH MICROSTRIP ANTENNA

When searching for a conformal, low profile antenna, one of the best choices is the microstrip antenna. This antenna is characterized by low cost and weight, ruggedness, ease of installation, and efficient radiation. Although the microstrip antenna has been around for over thirty years, very little work was published until the 1970's . During the early 1980's, much work has been done in furthering the development of the microstrip antenna. Thus far the microstrip antenna has seen most of its usage in the aviation community where low profile antennas are of utmost importance, but many other applications are being used as microstrip antenna theory is being improved.

While the microstrip antenna is a good choice for a low profile antenna, it does have one major disadvantage that limits its application. This drawback is narrow bandwidth. In recent years, several methods have been developed for improving the bandwidth as mentioned in Chapter I.

Microstrip antennas come in a variety of shapes and sizes, but one of the most commonly used is the rectangular half wavelength element. The element consists of a rectangular conducting sheet separated from a conducting ground plane by a thin dielectric as shown in Figure 2.1 The length is the most critical dimension and is slightly less than a half wavelength in the dielectric material as given in Equation 2.1. The width is not as critical, but is chosen less than a wavelength in the dielectric substrate to prevent higher order modes from being excited. The thickness, t is usually a fraction of a wavelength (typically $0.01\lambda_o$) and is generally defined by the thickness of commercially available printed circuit boards. [Ref. 4: p. 7-2]

$$L \sim 0.49\lambda_d = 0.49\lambda_o/\sqrt{\varepsilon_r} \qquad \text{(eqn 2.1)}$$

where

L = length of element,

ε_r = relative dielectric constant of printed circuit substrate, and

λ_o = free space wavelength.

13
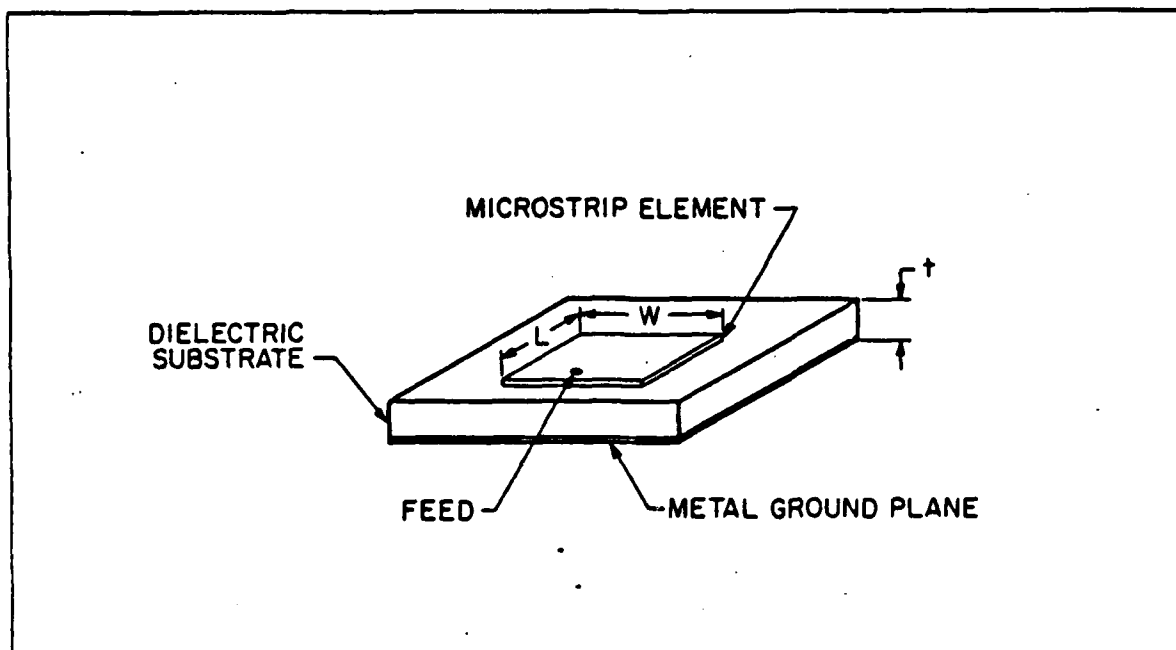
Figure 2.1   Rectangular Microstrip Antenna Element (from Ref. 4).

1. Input Impedance

Many models have been developed in order to predict the input impedance of the microstrip antenna. One of the simplest yet most enduring utilizes transmission line theory. This method models the microstrip as two parallel radiating slots connected by a low characteristic impedance transmission line as shown in Figure 2.2. The fields excited in the slots are 180 degrees out of phase between the edges. At resonance, the input resistance of the slots combine in parallel for an input resistance given in Equation 2.2. [Ref. 4: p. 7-3]

$$R_r = 60\lambda_o / W \qquad \text{(eqn 2.2)}$$

where

λ_o = the free space wavelength, and

W = the width of the microstrip element.

The resonant resistance for a microstrip antenna typically varies between 100 and 200 ohms. In order to match a half wavelength microstrip antenna to 50 ohms, the input resistance can be reduced by simply insetting the feed point location toward the center of the element. The resonant input resistance of a microstrip with an inset feed can be found from Equation 2.3 [Ref. 5: p. 12]

14

$$R_r = R_{re}\cos^2(\pi y_o/W) \qquad \text{(eqn 2.3)}$$

where

R_{re} = the input resistance for the edge fed micropatch, and

y_o = length of feed inset.
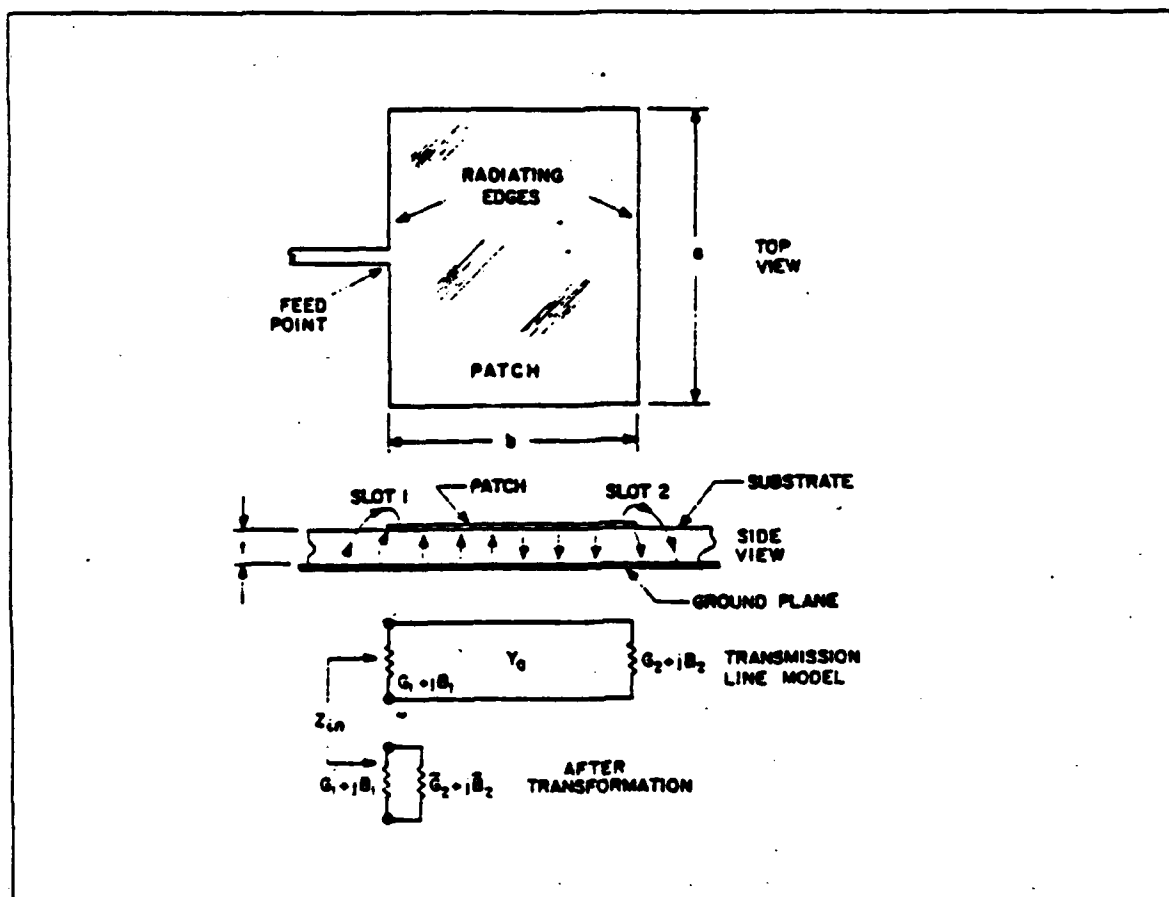
Figure 2.2   Transmission Line Model of Rectangular Microstrip Antenna
(from Ref. 5).

The input impedance of a rectangular microstrip antenna appears as approximately a circle on a Smith chart. Figure 2.3 shows the input impedance of a 4.14x6.858 cm microstrip for edge feed and inset feed (y_o = 1.016 cm) as reported by Carver and Mink. [Ref. 5: p. 13]

The bandwidth of an antenna can be defined in terms of several parameters such as input impedance, radiation efficiency, power gain, beamwidth, beam direction,

15

polarization, or sidelobe level [Ref. 6: p. 142]. In terms of input impedance, an antenna with a VSWR of 3:1 or less is an acceptable antenna. As shown in Figure 2.3, a rectangular microstrip antenna has a VSWR of 3:1 for a very small number of frequencies.
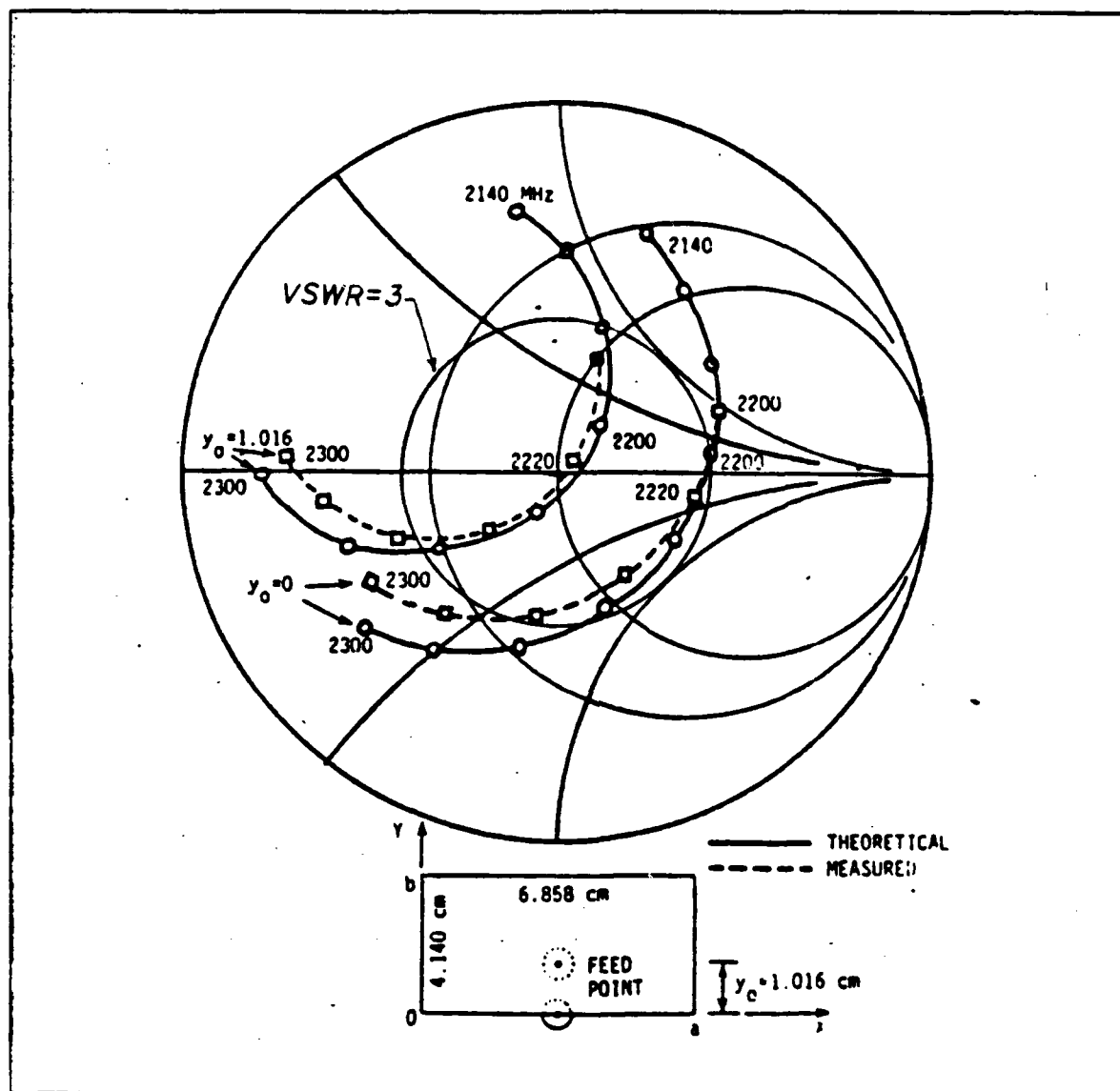
Figure 2.3   Measured and Calculated Impedance Curves for a Rectangular Microstrip Antenna (from Ref. 5).

2. Radiation Pattern

The microstrip antenna is an efficient radiator despite its low profile. Radiation patterns can be accurately calculated since the source of radiation is the small gap between the element and the ground plane. The primary radiation is horizontally polarized for an element parallel to the xy plane and is given by Equation 2.4 for a resonant antenna. [Ref. 4: p. 7-7]

$$E_{phi} = K \cos(\pi/2\sqrt{\varepsilon_r}\cos\theta) \quad \text{for} \quad (-\pi/2 \leq \theta \leq \pi/2) \qquad \text{(eqn 2.4)}$$

where

θ = the angle measured from the z axis ($\theta = 0$ is perpendicular to element), and

K = a constant.

Figure 2.4 shows the theoretical E-plane radiation pattern for a rectangular microstrip.

B. NON-RADIATING EDGES GAP-COUPLED MICROSTRIP ANTENNA

As discussed the rectangular microstrip antenna is an efficient radiator, but suffers from narrow bandwidth. One method for improving the bandwidth is to place additional radiators adjacent to a central rectangular element so that they are coupled by a narrow gap. These elements can be placed along the non-radiating edges, radiating edges, or along all four edges. The method chosen for this investigation is to place elements along the non-radiating edges. This configuration will be called the non-radiating edges gap-coupled microstrip antenna (NEGCOMA). The additional resonators can be of different lengths so that the staggering of resonant frequencies will yield a broader bandwidth as reported by Kumar and Gupta. [Ref. 1: p. 173]

In their report, Kumar and Gupta considered two additional resonators gap-coupled to the non-radiating edges of the rectangular microstrip antenna. For one central element different size gap widths were chosen (S_1, S_2) as well as different size resonator lengths (l_1, l_2) with the width remaining constant.

1. Input Impedance

The parameters that govern input impedance characteristics of the NEGCOMA are: gap width (S_1, S_2), length (l_1, l_2), and feed point location (a).

17
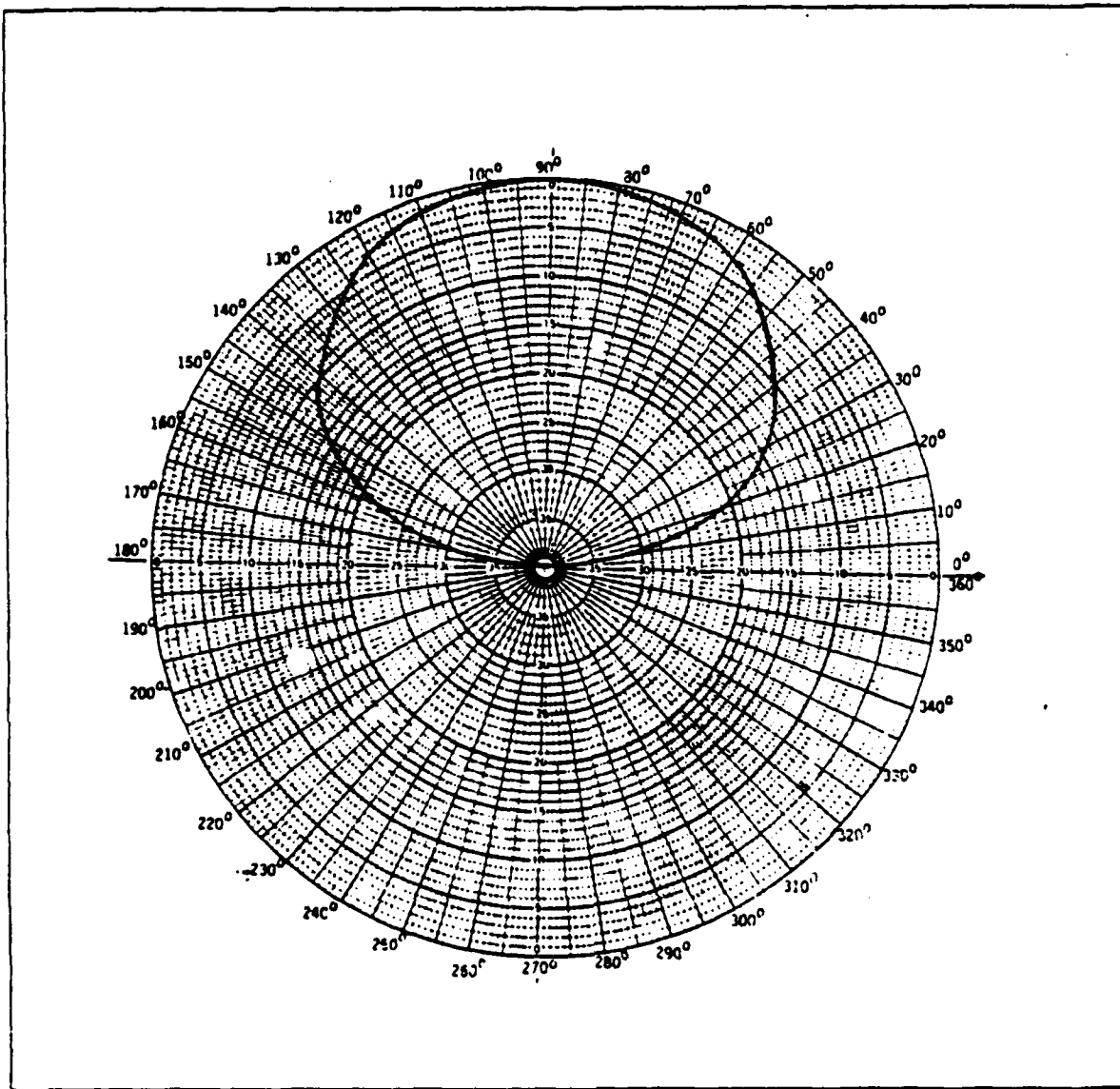
Figure 2.4   Theoretical E-Plane Pattern of Rectangular Microstrip Antenna
(from Ref. 4).

The input impedance loci for three different lengths of the coupled resonators ($l_1 = l_2 = 3.0, 2.9, 2.8$ cm) are shown in Figure 2.5 As the length of the parasitic element decreases, the loop in the impedance locus shifts downward and toward the left side of the Smith chart and corresponds to a higher resonant frequency. The size of the impedance loop can be controlled by the gap width. As the width is increased, the loop becomes smaller and shifts toward the right of the Smith chart. As the gap width is increased further, the impedance loop disappears and the impedance loci becomes similar to a rectangular patch microstrip.

18
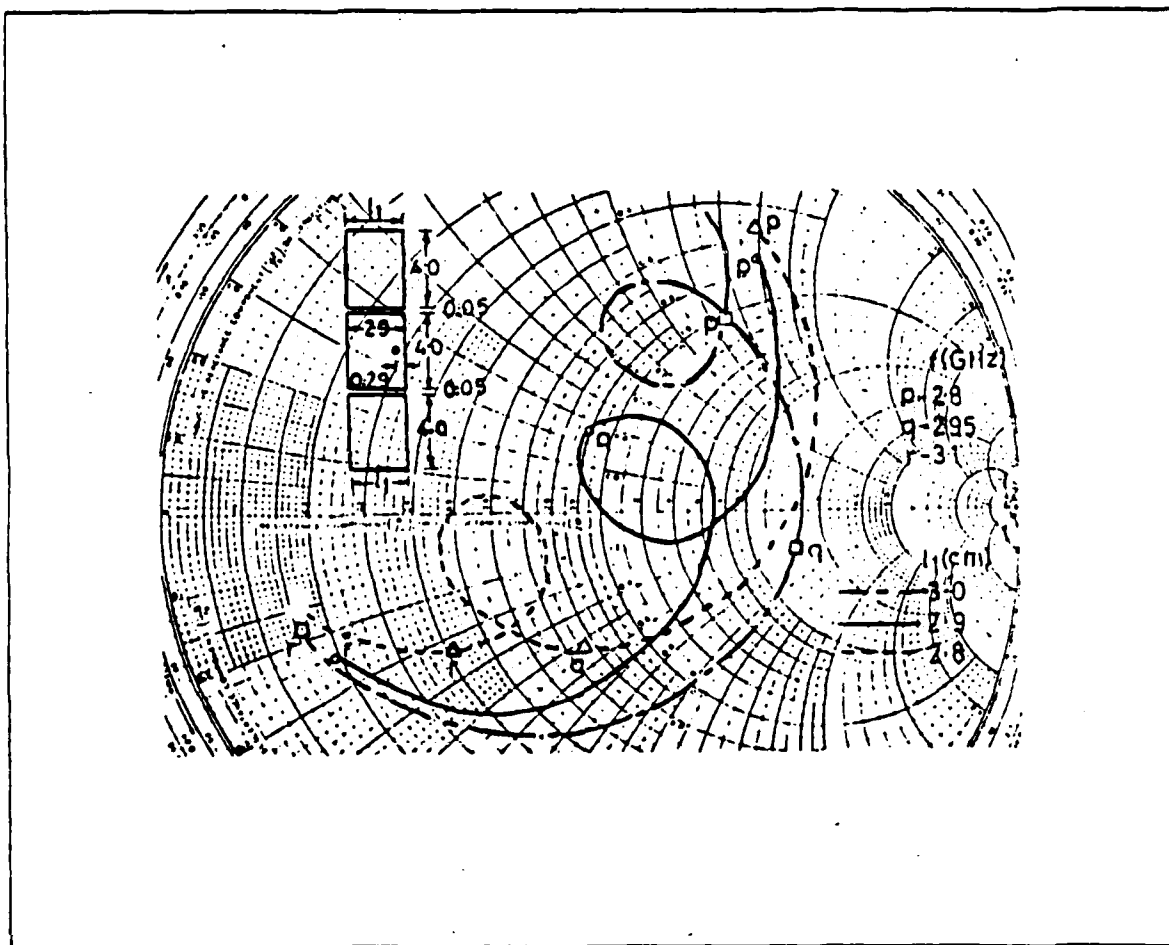
Figure 2.5   Input Impedance of NEGCOMA (from Ref. 1).

The effect of changing the feed point location is to lower the input impedance and shift the impedance loci toward the left side of the Smith chart just as in the case of the rectangular patch microstrip.

2. Radiation Pattern

Radiation patterns for a NEGCOMA with $l_1 = 2.8$ cm, $l_2 = 2.5$ cm, $W = 3$ cm, $S_1 = S_2 = 0.03$ cm, $h = 0.318$ cm, and $\varepsilon_r = 2.55$ for several frequencies are shown in Figure 2.6 Although the patterns display notches at various frequencies, due to the interaction between resonators, they follow the same general trend as a pattern from a rectangular microstrip antenna. Patterns from the NEGCOMA offer a nearly hemispherical coverage, with primary coverage overhead.
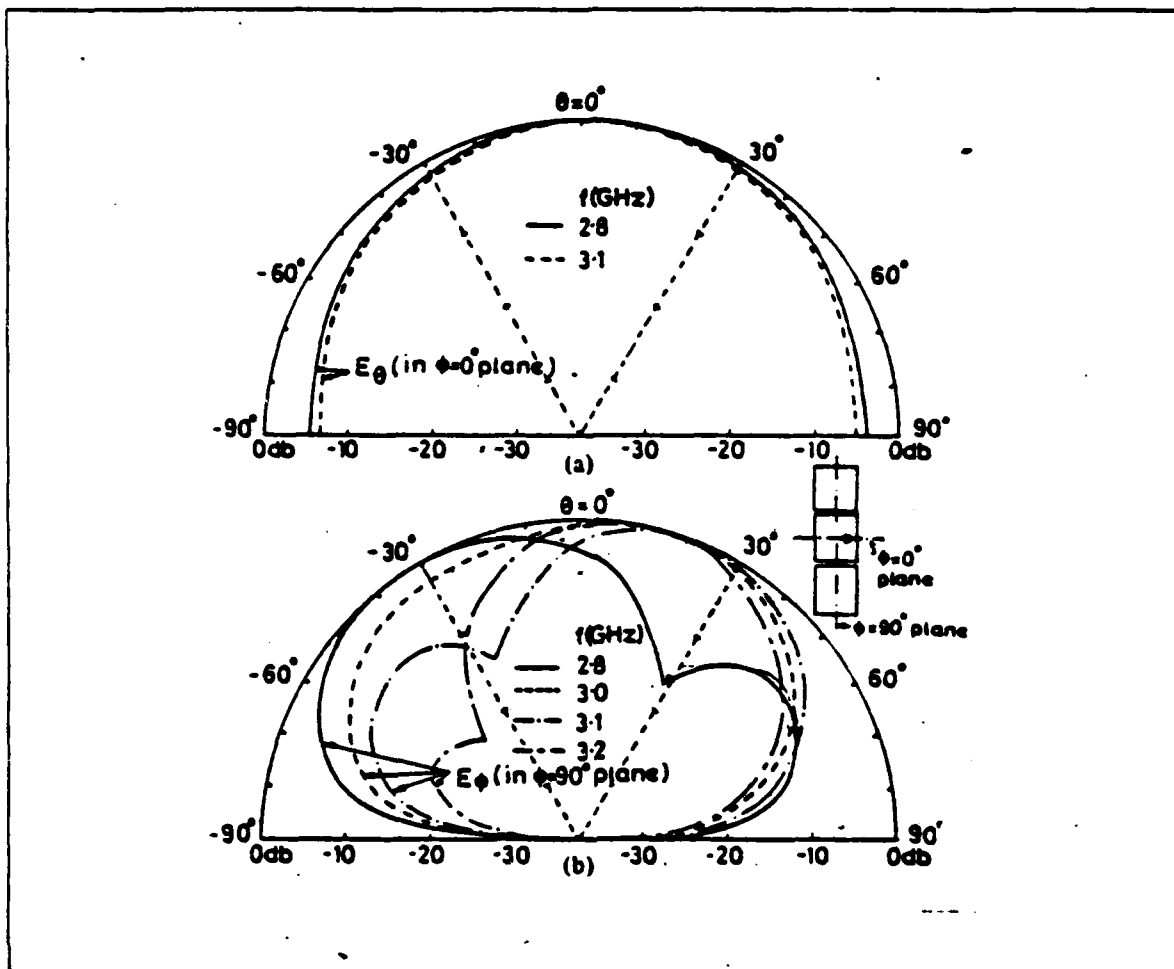
Figure 2.6 Radiation Patterns for NEGCOMA (from Ref. 1).

C. NUMERICAL ELECTROMAGNETICS CODE-METHOD OF MOMENTS COMPUTER MODEL

The Numerical Electromagnetics Code-Method of Moments (NEC-MOM) computer program is a user oriented code for the analysis of the electromagnetic response of antennas and other metal structures. The analysis is accomplished by the numerical solution of integral equations for induced currents. This approach is best suited to structures with dimensions up to several wavelength. While there is no theoretical size limit, large structure size relative to a wavelength could require more computer time and file storage than is practical. For structures that are small relative to a wavelength, NEC-MOM provides a highly accurate and versatile tool for electromagnetic analysis. [Ref. 7: pp. 1-13]

20

The basic devices for modeling structures are short straight segments for modeling wires and flat patches for modeling non-radiating surfaces. The main electrical consideration is segment length relative to wavelength. Generally, segment length should be less than about one-tenth wavelength. The radius of the wire should be chosen small relative to the segment length, typically less than one-half segment length. Other restrictions and guidelines are given in [Ref. 7] and should be followed for acceptable results.

1. Half Wavelength Microstrip Antenna Model

Wire grid modeling of conducting surfaces can be accomplished with reasonable accuracy as long as the wire grid spacing is dense enough to approximate the surface. Using guidelines presented by NEC-MOM a computer model of a simple microstrip antenna was developed for comparison with measured results before attempting to model a gap-coupled microstrip antenna.

The antenna selected for comparison was reported by Carver and Mink [Ref. 5: p. 13] and consists of 4.14 cm non-radiating sides, 6.858 cm radiating sides, and a relative dielectric constant equal to 2.5. The thickness was not given but will be assumed 0.159 cm (the height given for other examples is this article).

Since NEC-MOM cannot simulate the dielectric constant of the substrate, all dimensions were converted from waveguide wavelength to free space wavelength dimensions at 2.2 GHz. In other words, each dimension was multiplied by $\sqrt{\varepsilon_r}$ to produce an equivalent air dielectric microstrip element. The result is a 7x11 cm microstrip with height equal to 0.25 cm. The wire grid structure used to simulate this antenna is shown in Figure 2.7 The wire grid spacing is 1 square cm.

Figure 2.8 shows a plot of the input impedance for the rectangular microstrip antenna and the wire grid model. Although not an exact duplication, the wire grid model follows the impedance curve of the dielectric patch reasonably well.

Figures 2.9 and 2.10 show the radiation pattern for the wire grid microstrip antenna. As predicted the major portion of the radiation is the horizontally polarized field.

2. Non-radiating Edges Gap-Coupled Microstrip Antenna

After determining that a simple rectangular microstrip antenna could be modeled reasonably well using NEC-MOM, attempts were made to duplicate a non-radiating edges gap-coupled microstrip antenna. The antenna chosen had dimensions of $L = 2.9$ cm, $W = 4$ cm, $l_1 = l_2 = 2.9$ cm, $S_1 = S_2 = 0.05$ cm, and feed point location inset

21
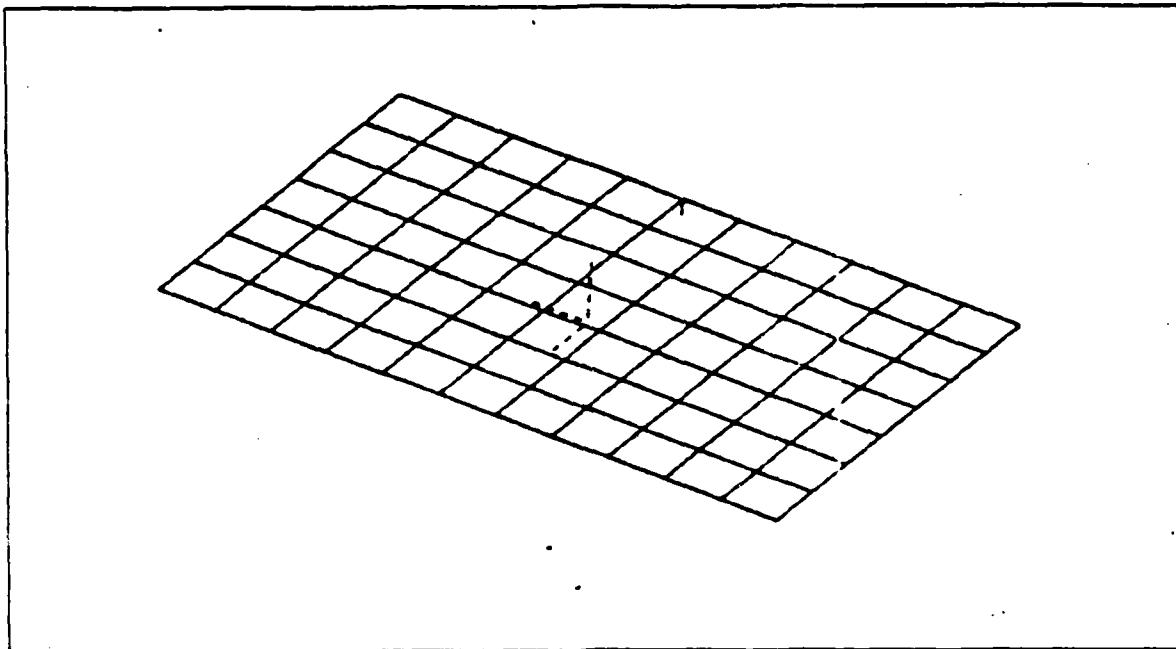
Figure 2.7   Wire Grid Model of Rectangular Microstrip Antenna.

0.29 cm. After converting these dimensions to equivalent dimensions for air dielectric, a NEGCOMA model of size $L = 4$ cm, $W = 6$ cm, $l_1 = l_2 = 4$ cm, $S_1 = S_2 = 0.08$ cm, and feed point location inset 0.5 cm was developed. Figure 2.11 shows the wire grid model. The resulting impedance loci occurred farther to the right with a much smaller impedance loop than the antenna reported by Kumar and Gupta. In order to achieve approximately the same results as Kumar and Gupta, the gap widths S_1, S_2 were reduced to 0.05cm. The input impedance for this antenna agreed with measured results and is shown on Figure 2.12. Figure 2.13 shows a plot of VSWR in the frequency range of interest for the NEGCOMA and the rectangular element without additional resonators. For a VSWR of less than three, the single rectangular element has a 170 MHz bandwidth, while the NEGCOMA has a 400 MHz bandwidth, an increase of 2.35 times. This configuration of the NEGCOMA has an impedance bandwidth of approximately 13 percent which is still quite small for a shipboard antenna. This bandwidth could possibly be improved by changing the resonator size, location, and/or height.

Radiation patterns for the NEGCOMA wire grid model are shown on Figures 2.14-2.19. These patterns also follow the general trend of a rectangular microstrip antenna, with irregularities caused by the interaction of the additional resonators. The

22
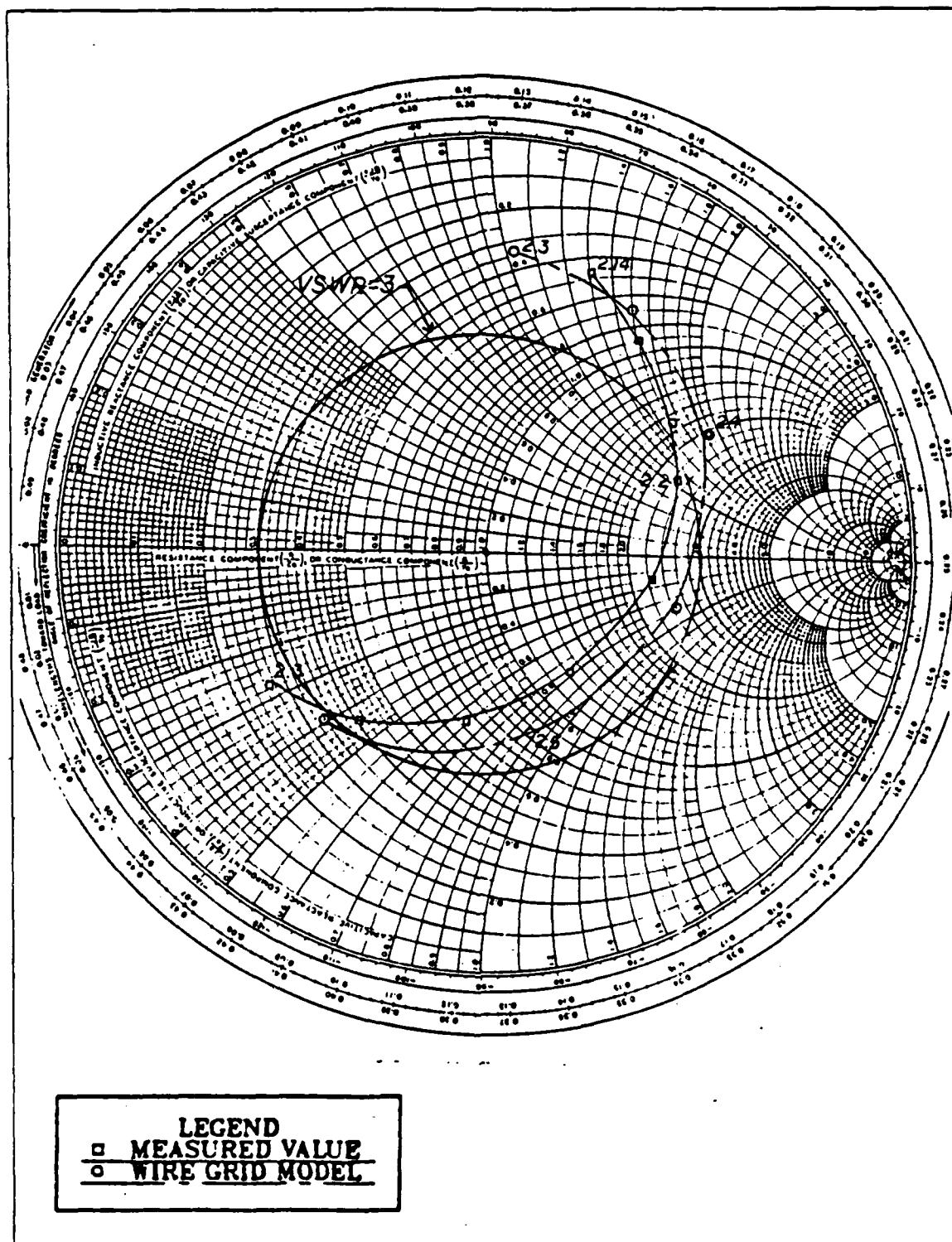
Figure 2.8   Smith Chart Impedance Plot of Rectangular Microstrip
and Wire Grid Model.

23
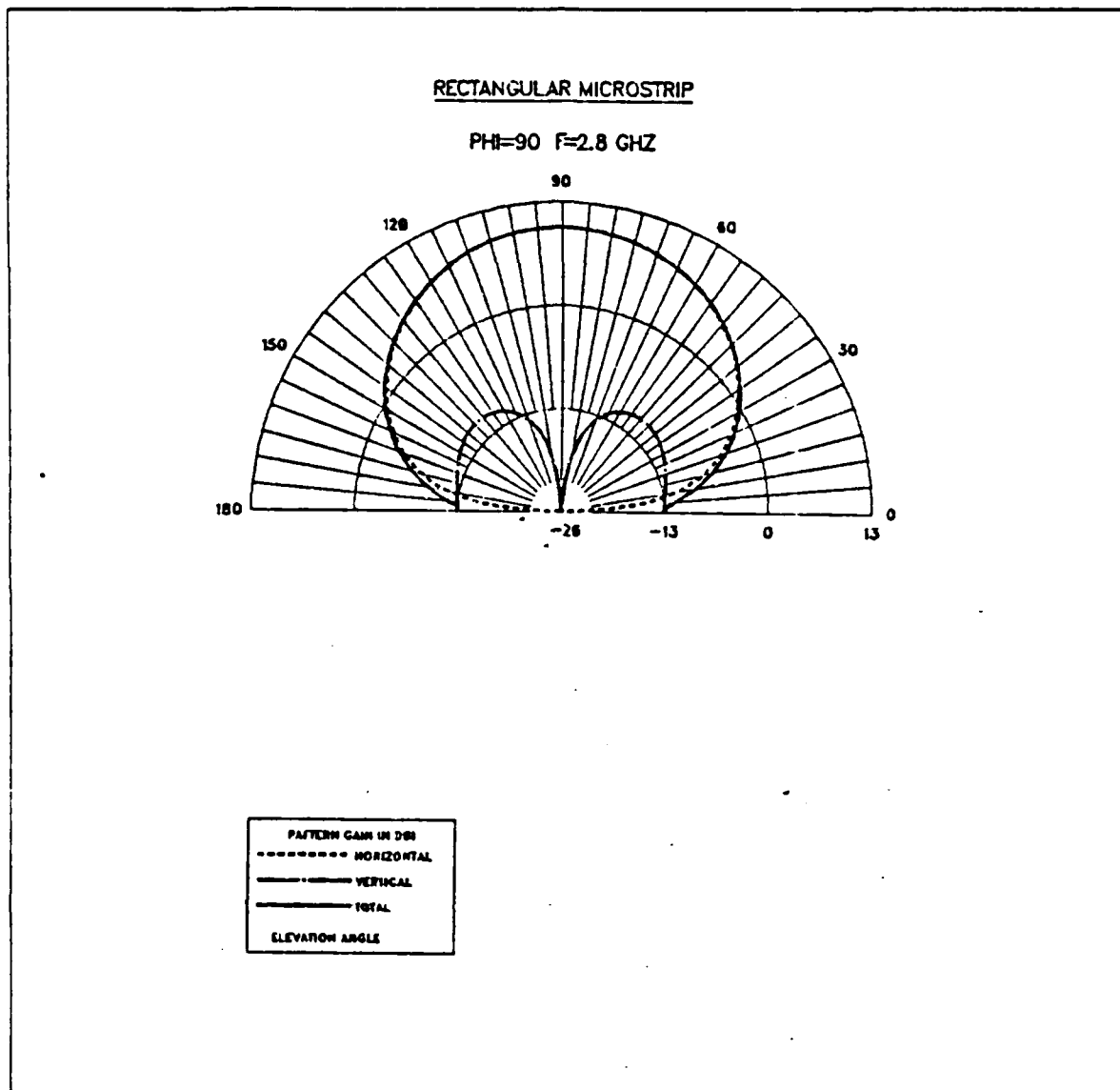
Figure 2.9   Radiation Pattern for Rectangular Wire-Grid Model
$\varphi = 90$, F = 2.8 GHz.

patterns show almost hemispherical coverage with wider coverage for higher frequencies.

The NEGCOMA used in this example was sized for an operating frequency of 3 GHz. If the antenna was designed for 300 MHz, the overall size would be approximately 0.88x0.4 meters, assuming a dielectric of 2.5.

24
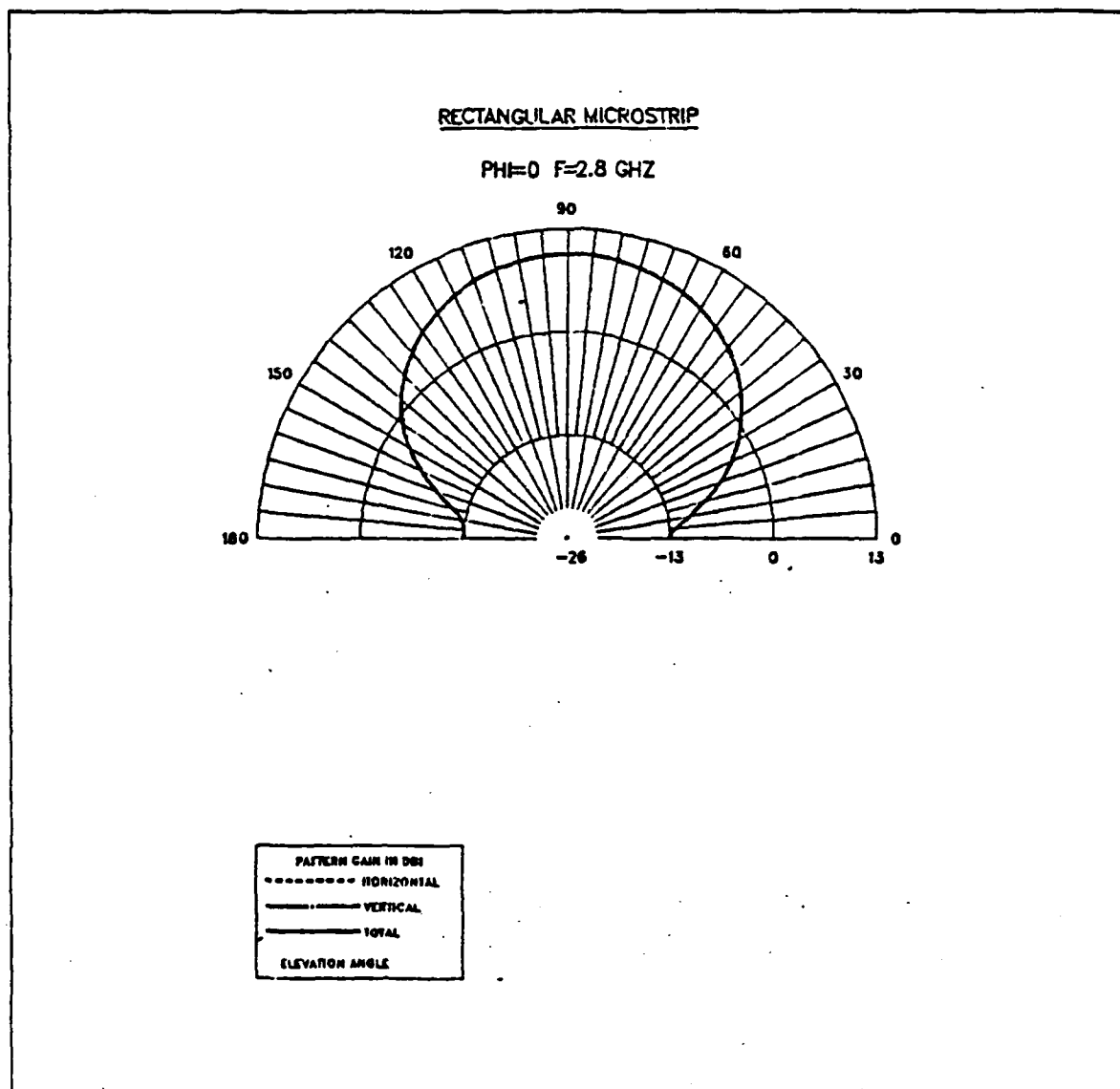
Figure 2.10   Radiation Pattern for Rectangular Wire-Grid Model
φ = 0, F = 2.8GHz.
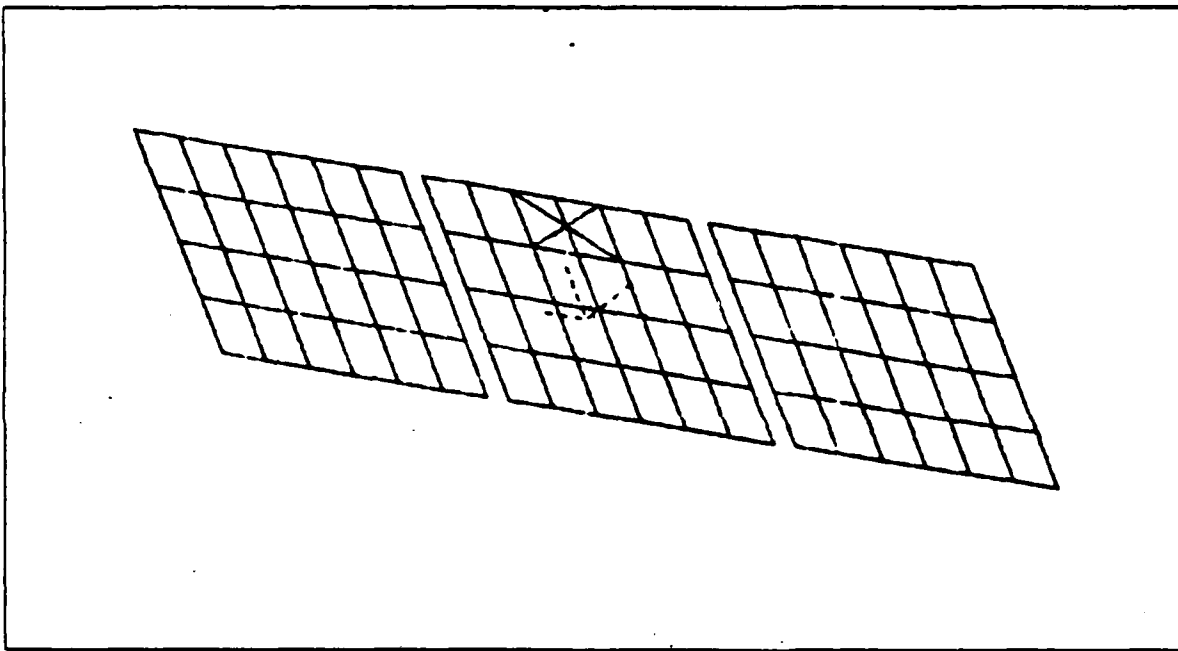
Figure 2.11   Wire Grid Model of NEGCOMA.
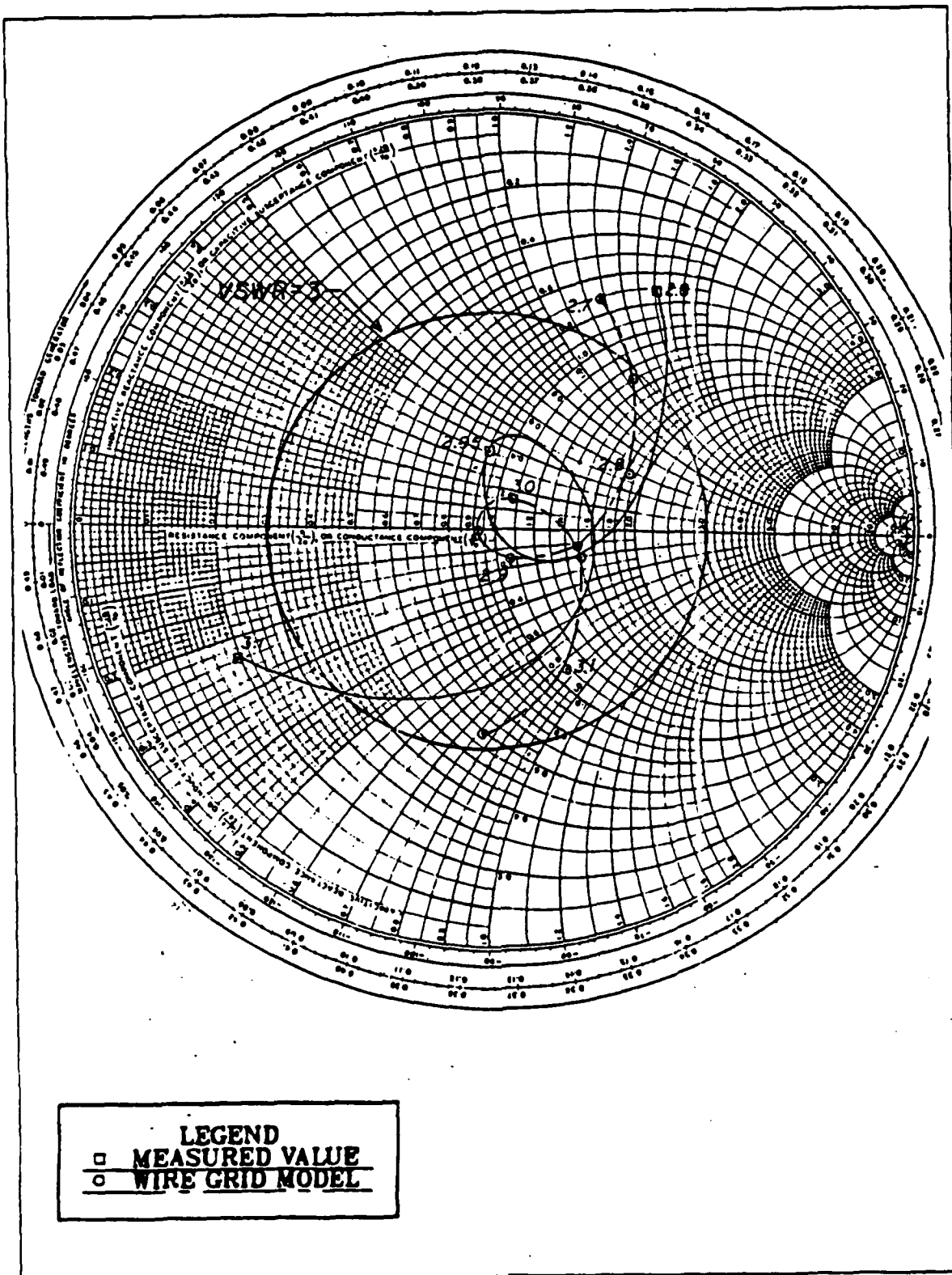
Figure 2.12   Smith Chart Impedance Plot of NEGCOMA.
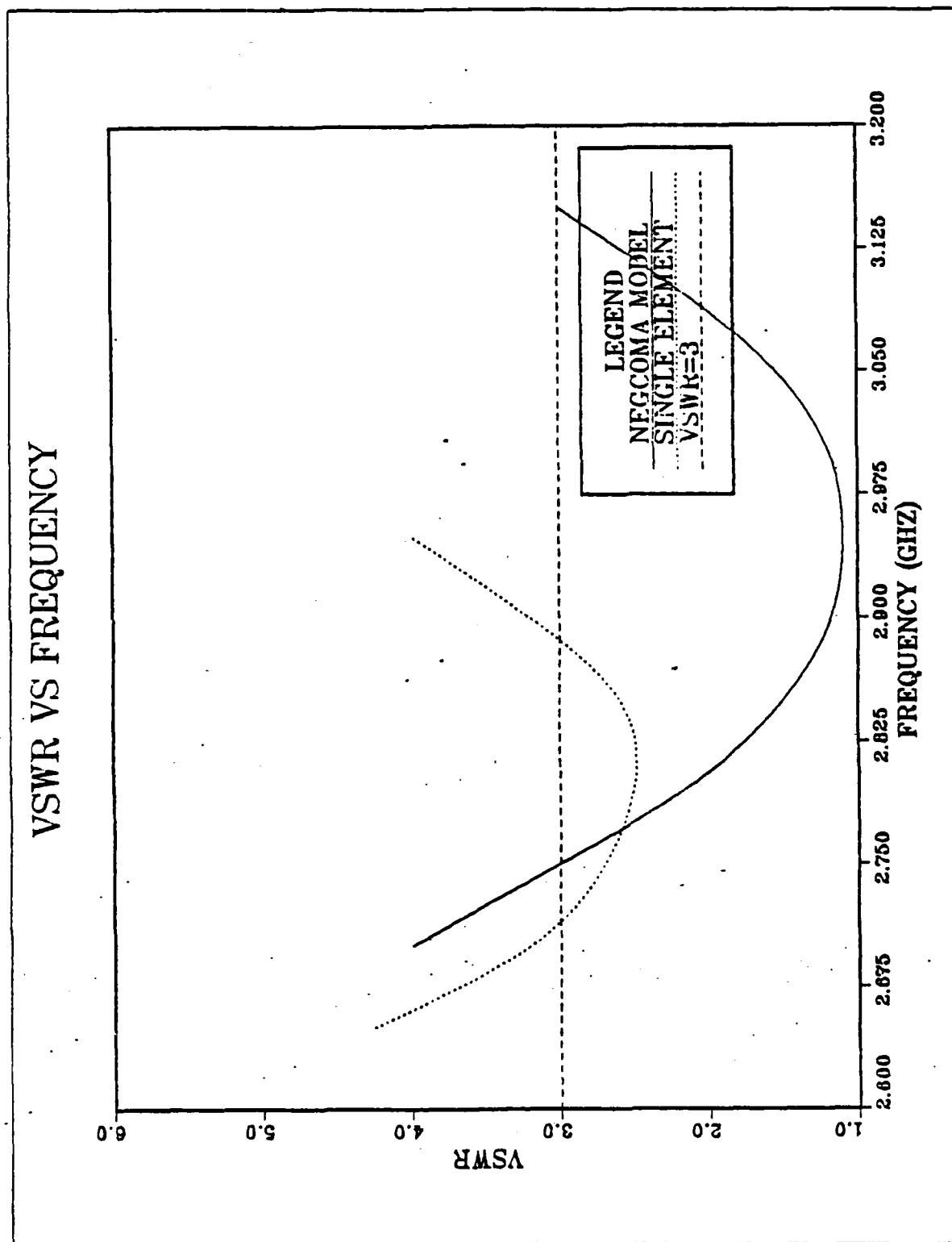
Figure 2.13   VSWR vs. Frequency for NEGCOMA and Rectangular Microstrip
Antenna.

28
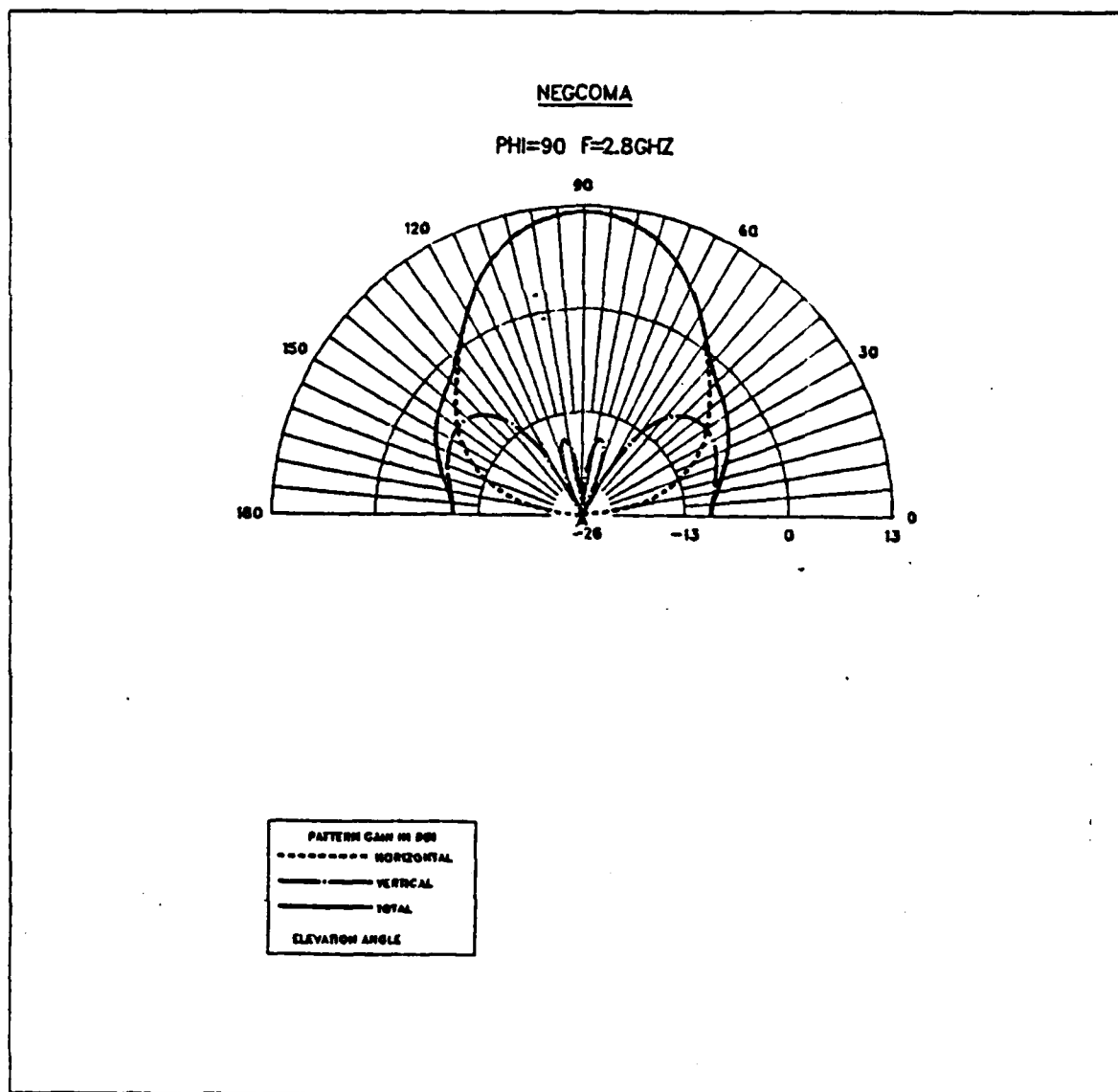
Figure 2.14 Radiation Pattern for NEGCOMA Wire-Grid model, φ = 90, F = 2.8 GHz.

29
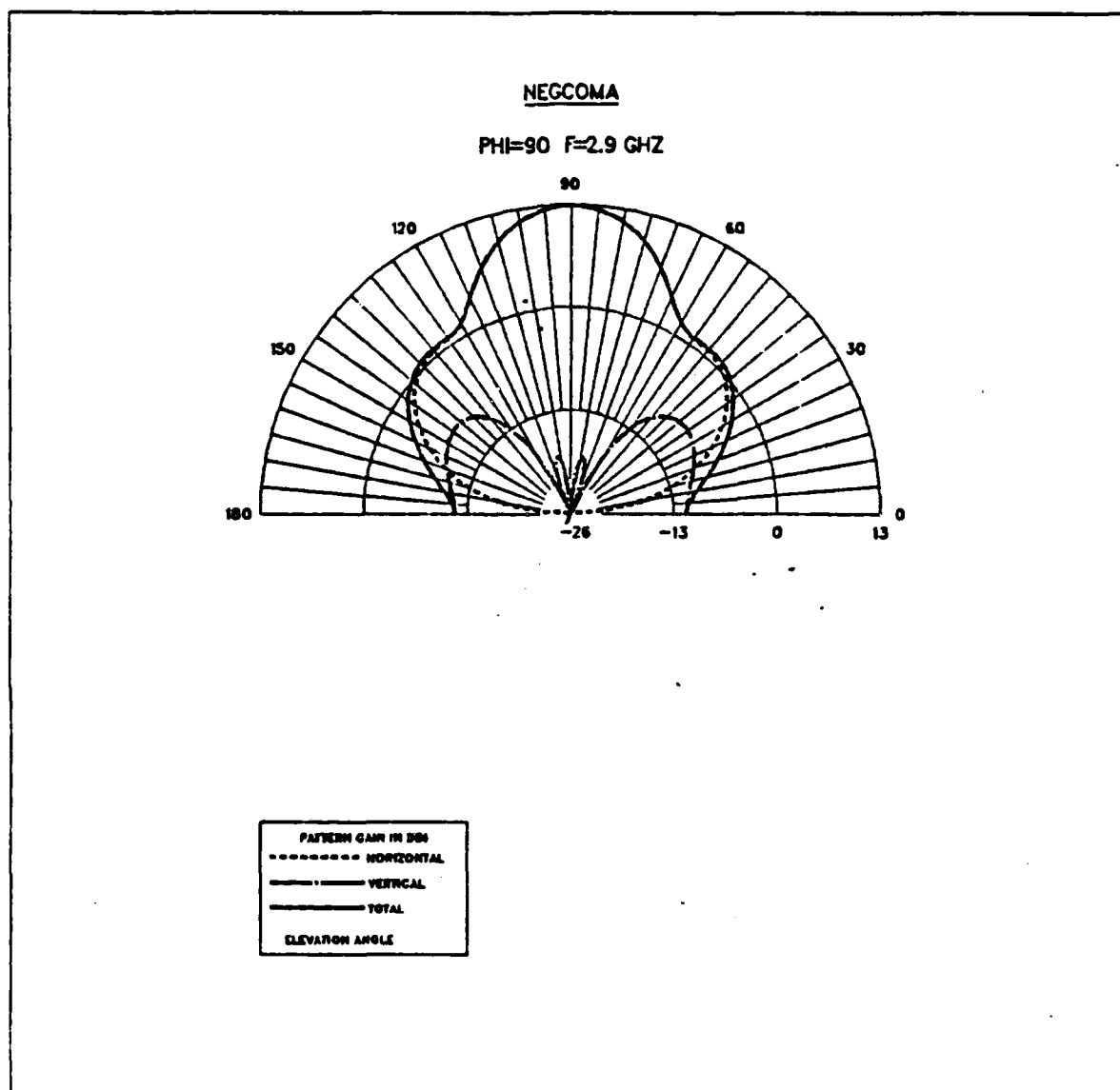
Figure 2.15   Radiation Pattern for NEGCOMA Wire-Grid model, φ = 90, F = 2.9 GHz.
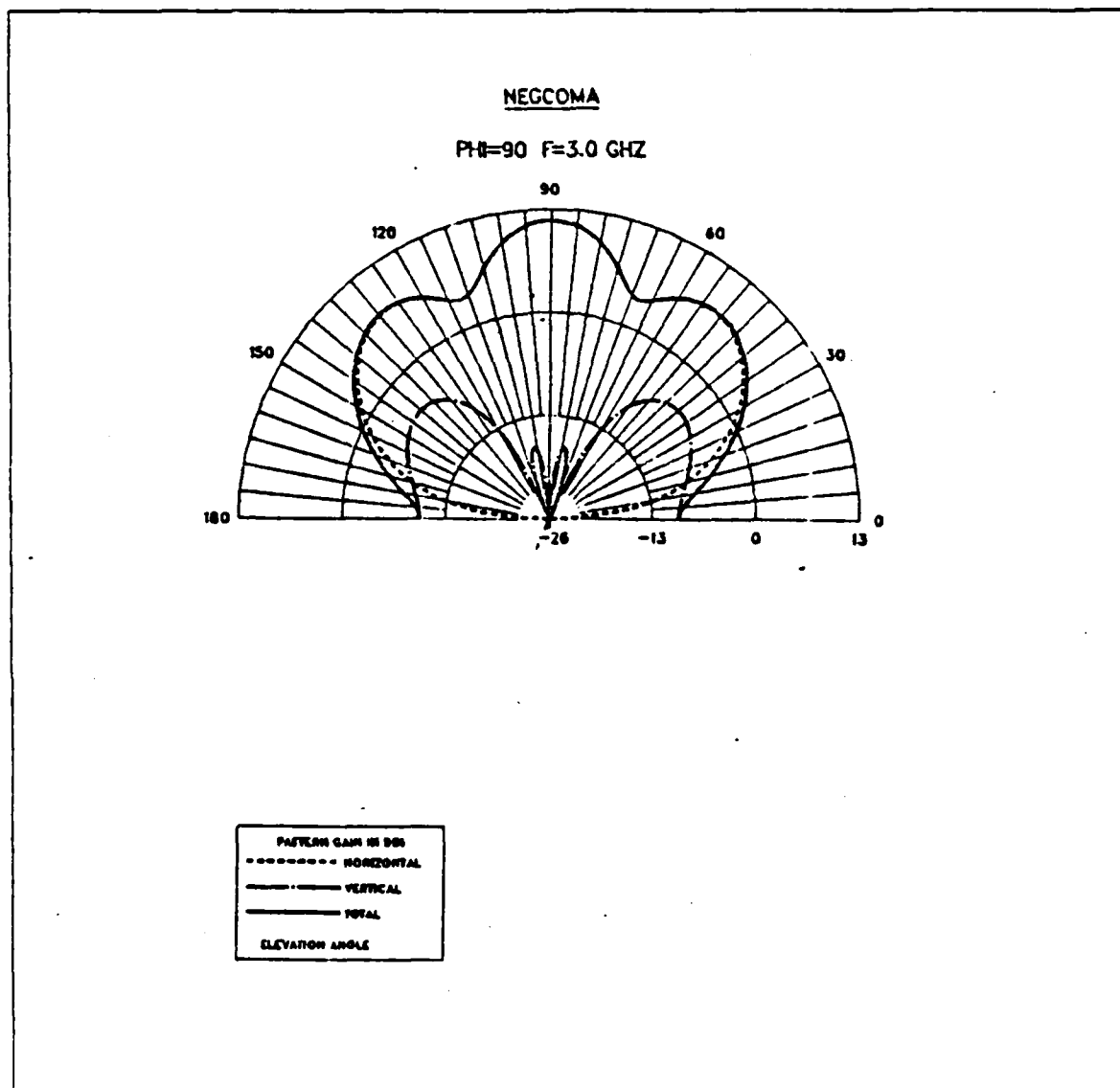
Figure 2.16 Radiation Pattern for NEGCOMA Wire-Grid model, $\varphi = 90$, F = 3.0 GHz.
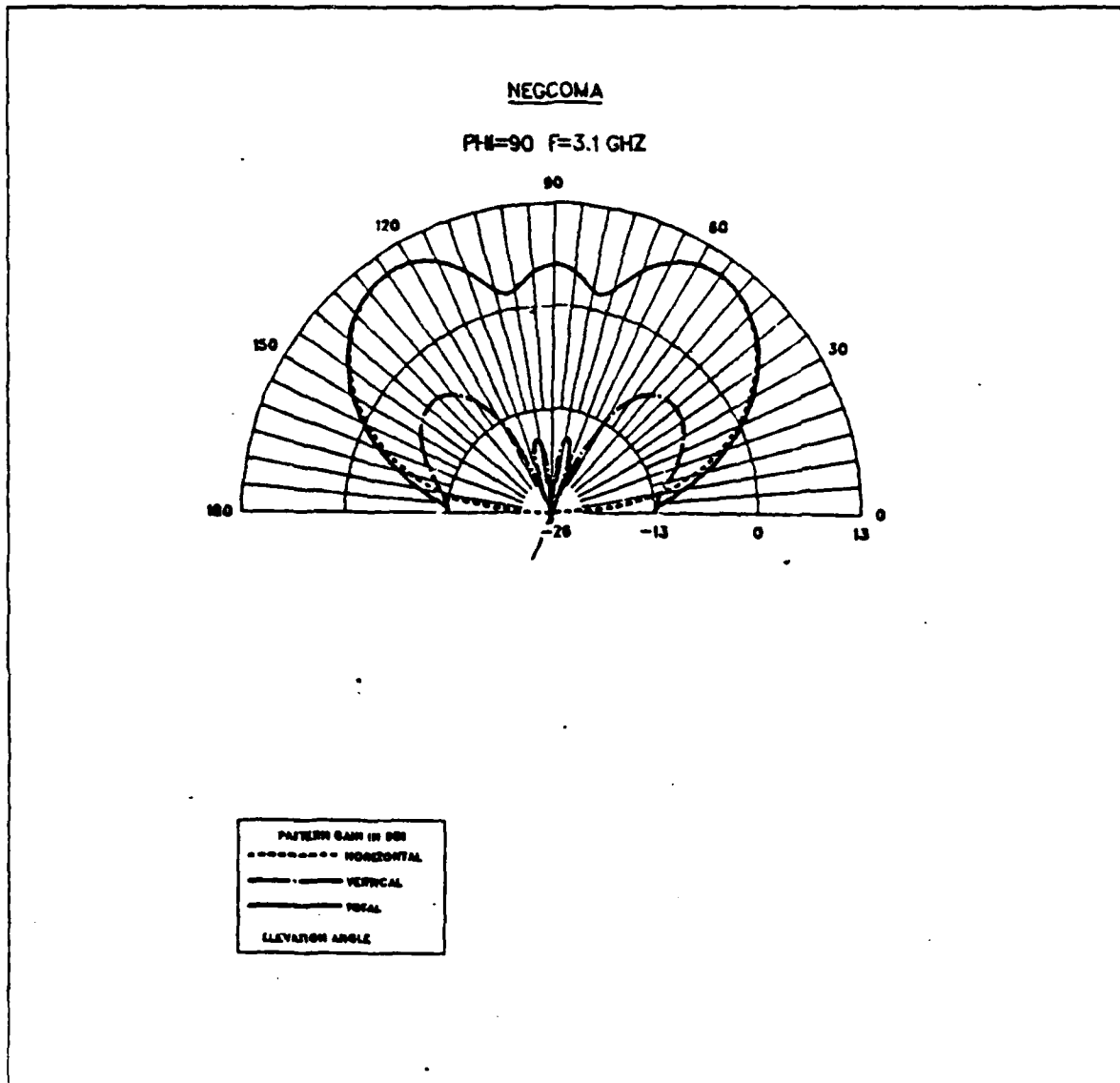
Figure 2.17   Radiation Pattern for NEGCOMA Wire-Grid model, $\varphi = 90$, F = 3.1 GHz.
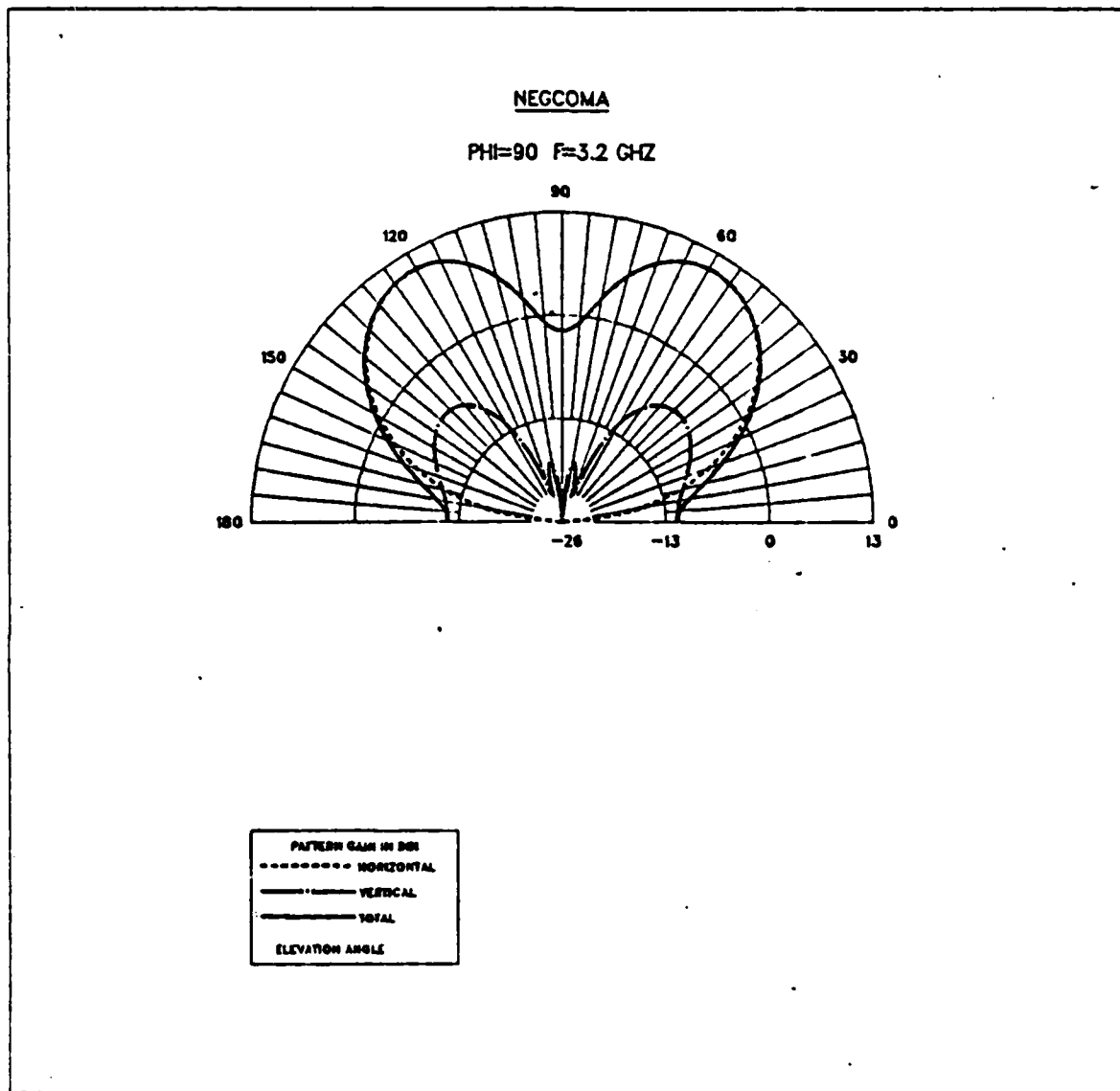
Figure 2.18   Radiation Pattern for NEGCOMA Wire-Grid model, φ = 90, F = 3.2 GHz.
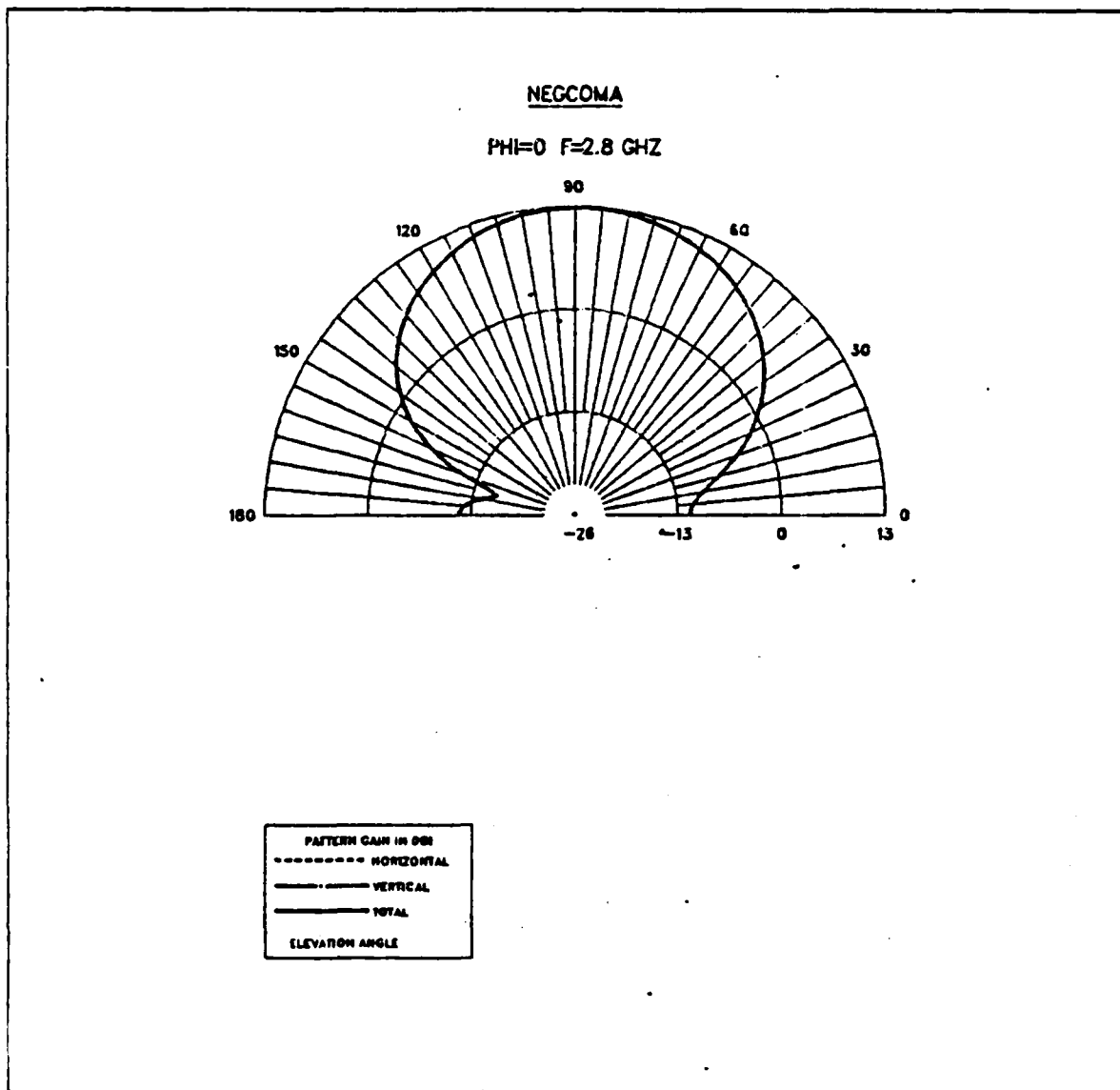
Figure 2.19   Radiation Pattern for NEGCOMA Wire-Grid model, φ = 0, F = 2.8 GHz.

III. CROSSED-SLOT ANTENNA

A. RIDGED-CAVITY CROSSED-SLOT ANTENNA

A slotted antenna in its basic form is an opening cut into an extended metallic sheet of metal. The slot can be excited by a voltage source such as a parallel transmission line or coaxial transmission line. Radiation patterns can be determined by the currents on the conducting sheet or more simply by considering the fields of a complementary structure. Booker's [Ref. 8] extension of Jacques Babinet's principle shows that the field of the slot can be deduced from those surrounding a dipole of the same dimensions by interchanging the electric and magnetic vectors.

Although a slotted antenna has radiation patterns similar to a dipole, it suffers from a very narrow impedance bandwidth. In order to increase the impedance bandwidth, a more practical case of a slotted antenna must be considered, a cavity-backed slot. The impedance bandwidth of a cavity-backed slot is still narrow, but can be increased at the expense of greater cavity volume [Ref. 9: pp. 96-97].

A cavity-backed slot antenna is a cavity resonator which radiates from the slot aperture. The field distribution in the slot is dependent on the excitation of higher cavity modes as well as the principle TE_{10} mode. In order to obtain the maximum radiation conductance, the energy stored in the cavity near the slot must be primarily in the TE_{10} mode. This is accomplished by making the dimensions of the cavity large enough so that the dominant mode is above cut off.

An important design parameter is the antenna Q which is related to the amount of energy stored in each mode. When Q is minimized, the stored energy is primarily in the dominant mode and the antenna impedance bandwidth is increased. [Ref. 4: pp. 8-20,8-21]

Circular polarization can be achieved by placing two slots perpendicular to each other to form a cross. Increased bandwidth can be achieved by lengthening the slots to a point where a low value of Q is encountered. A crossed-slot antenna has been built with the following dimensions:

- cavity edge 0.65λ
- cavity thickness 0.08λ
- slot length 0.915λ

The measured 2:1 VSWR bandwidth of this antenna was 20.8 percent. [Ref. 9: p. 123]

35

In order to achieve further increase in bandwidth, King and Wong [Ref. 2: pp. 687-689] added stepped ridges to the cavity of a crossed slot antenna. Their objective was to develop a wideband hemispherical-coverage antenna with an operating frequency range from 240 to 400 MHz. The experimental antenna used by King and Wong was approximately half scale therefore frequency measurements were made from 580 MHz to 800 MHz.
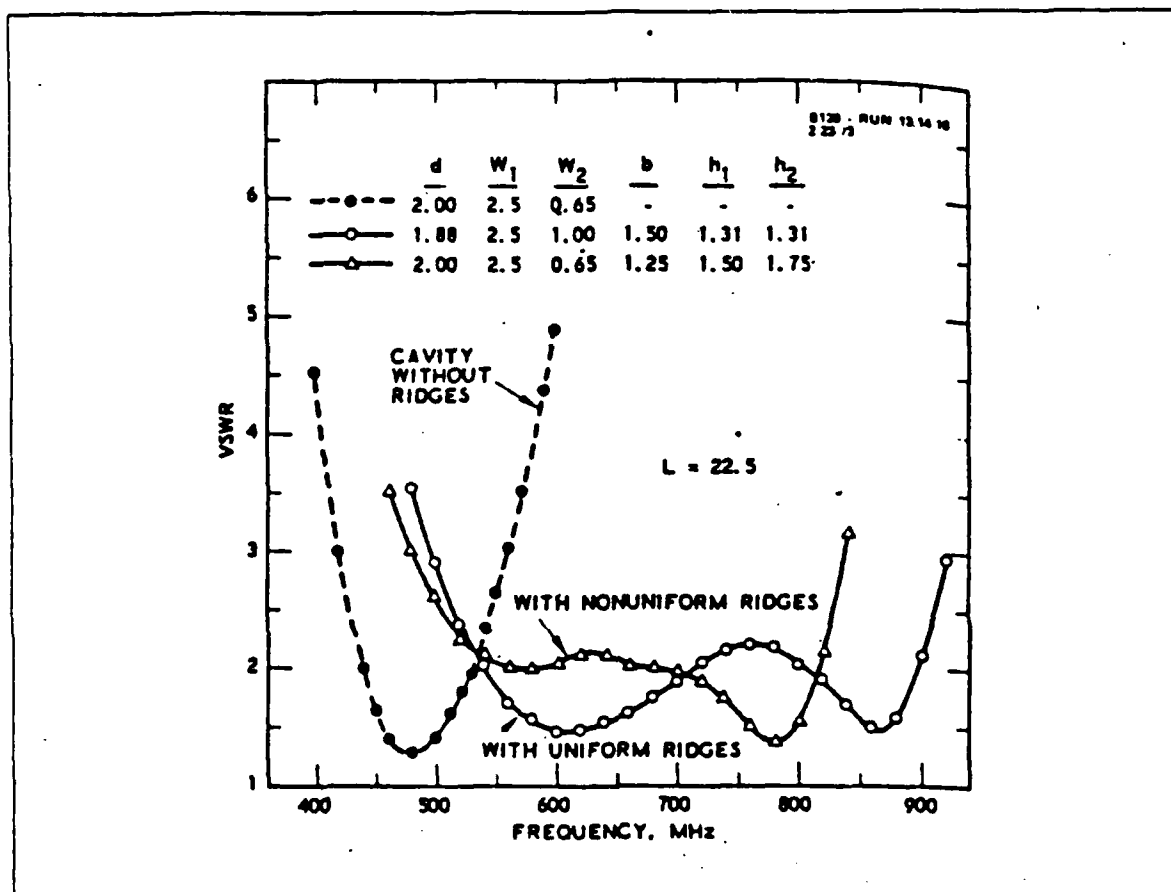
Figure 3.1   VSWR Response of Cavity-Slot Antenna With and Without Ridges
(from Ref. 2).

Voltage standing wave ratio measurements were made for a variety of slot and cavity configurations. From their data, King and Wong determined that the slot length and width and the cavity depth influence the resonant frequency of the antenna. A narrower or longer slot or deeper cavity lowers the resonant frequency. The VSWR response could be made flatter by making the slots nonuniform or by stepped ridges in

36

the cavity. Figure 3.1 compares the VSWR response of a cavity without ridges with that of a ridged cavity.

Radiation pattern measurements were made for the nonuniform ridge configuration. The radiation from this antenna was circular overhead and linear near the horizon. The 3-dB beamwidth varied from 120 degrees at the low frequency range to about 40 degrees at the high frequency range demonstrating that the pattern response of the antenna is wideband.

B.   NUMERICAL ELECTROMAGNETICS-BASIC SCATTERING CODE

The Numerical Electromagnetics Code-Basic Scattering Code (NEC-BSC) [Ref. 10] is a user-oriented computer code for analyzing radiation from antennas using the Geometrical Theory of Diffraction (GTD). The code can be used to predict far zone patterns, to provide coupling between antennas, and determine potential radiation hazards.

Because of the ray optical techniques used to determine components of the field incident upon and diffracted by the various structures, only the most basic features of a complex structure need be modeled.

There are two basic scattering elements available to NEC-BSC, an arbitrary sided plate and a finite elliptic cylinder. A number of these elements can be placed in proximity to simulate a complex structure such as a ship's superstructure, an aircraft fuselage, or any other environment where an antenna is to be mounted. The code does have the limitation that each plate should have edges at least a wavelength long and cylinder major and minor radii and length be at least a wavelength.

The NEC-BSC can model large structures as illuminated by a source antenna such as a dipole or slot. The sources can be modeled as a single element or grouped together as an array. Source types can be specified as electric or magnetic with a uniform, piecewise sinusoidal, or TE_{01} source distribution. The code requires that antennas be mounted on flat plates vice cylinders and be at least a wavelength from all plate edges.

The output listing from the NEC-BSC is divided into two main sections. The first section provides information on how the code interpreted the input data; listing source type and dimensions, pattern cut in the near or far field as requested, and scattering component and source location as referenced to the input coordinate system. The second section gives tabulated data for the field patterns. For the far zone case this includes the angular position (θ,φ), magnitude of the electric field (E_{theta}, E_{phi}), phase of electric field, and radiation intensity U in dB as given by Equation 3.1.

37

$$U = R^2 |E|^2 / (2Z_o) \qquad \text{(eqn 3.1)}$$

where

R = far zone distance,

E = electric field, and

Z_o = free space impedance.

If directive gain is required, the power radiated by the antenna must be calculated external to the code and supplied in the input section. This section of the output also tabulates the major component of radiation intensity, minor component, axial ratio, and polarization sense.

The NEC-BSC is not directly supported with plotting routines, but routines are available at NPS to plot the antenna geometry and radiation patterns [Ref. 11]. Figures 3.2-3.4 show typical output plots for a half wavelength slot on a flat plate. To obtain the total E-field on the rectangular plot format as in Figure 3.3, three separate plots are required, one for E_{theta}, one for E_{phi}, and one for E_{peak}. For vertical cut patterns theta is varied with phi held constant at the selected value. Horizontal cut patterns are generated by holding theta constant and varying phi. For the purposes of this paper, horizontal cut patterns will be generated directly over the plane of the antenna (around the z-axis with respect to the input coordinate system) with theta equal to 90 degrees.

C.   COMPUTER MODEL OF CROSSED SLOT ANTENNA

The slotted antenna as modeled by the NEC-BSC only radiates on one side of a plate. This precludes modeling an antenna such as the ridged-cavity crossed-slot. Although the ridged-cavity crossed-slot cannot be modeled, using NEC-BSC, this section will show that a simple crossed-slot antenna has acceptable radiation patterns and would be an excellent candidate for shipboard mounting.

The radiation from the single slot antenna is linearly polarized for vertical cut patterns and elliptically polarized for horizontal cut patterns. As stated, elliptical polarization can be achieved by placing two slots on a plate to form a cross. Better hemispherical coverage can be obtained if there is a 90 degree phase shift between their inputs, similar to feeding two orthogonal center-fed dipoles with 90 degree phase shift [Ref. 12: p. 748]. Figure 3.5 shows a crossed-slot antenna on a 4x4 meter flat plate.

38

HALF WAVE SLOT AT 300 MHZ
viewing point φ = 0.00 deg
θ = 0.00 deg
r = 20.00 m

$\phi = 0$

X in m

Y in m
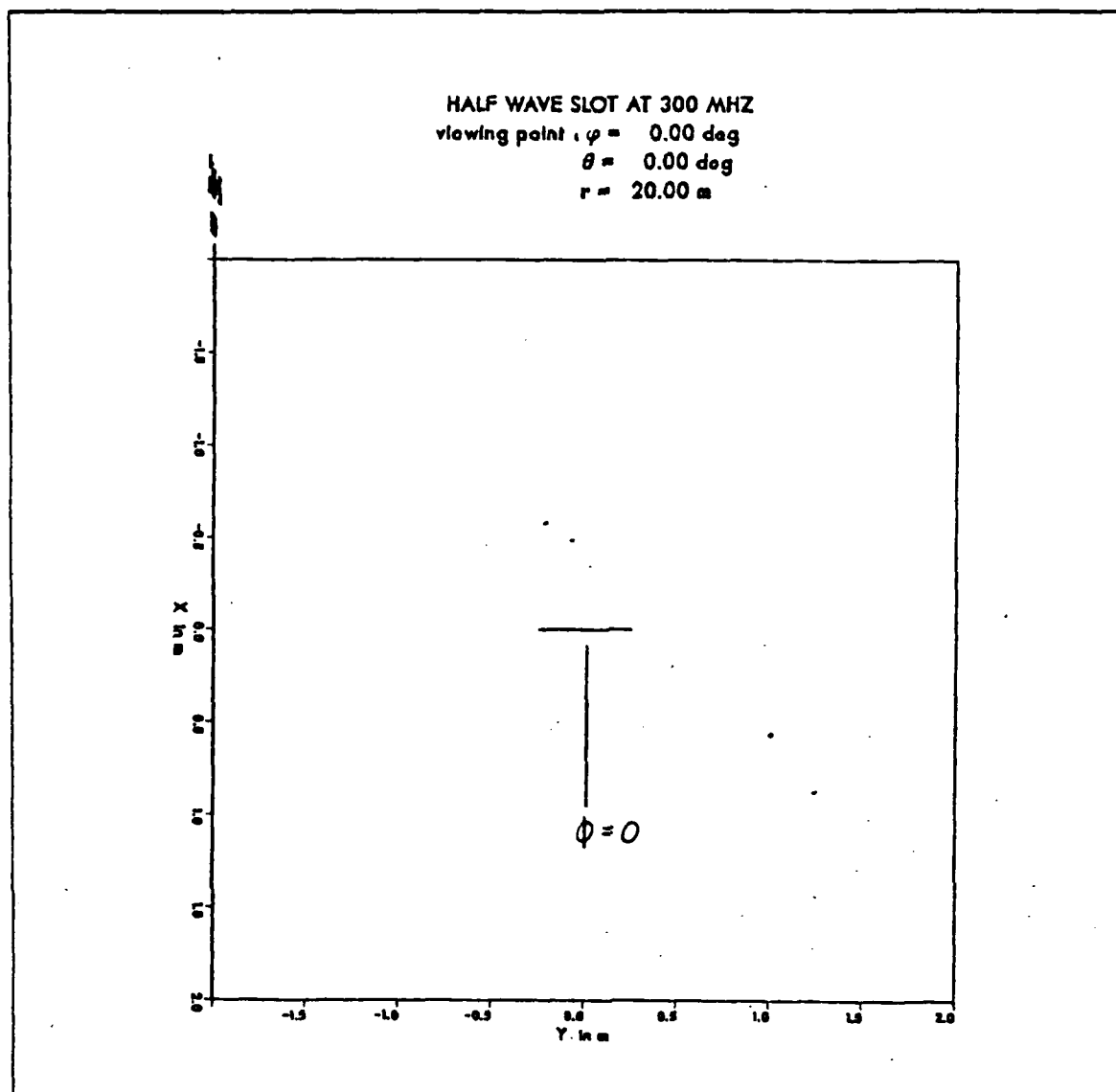
Figure 3.2 Half Wavelength Slot at 300 MHz on 4x4 Meter Flat Plate.

Figures 3.6 and 3.7 show the horizontal and vertical cut radiation patterns for this antenna with one slot fed at 90 degrees with respect to the other.

As mentioned, the strength of the NEC-BSC is its ability to model an antenna in a complex environment. Figure 3.8 shows a partial profile and plan view of a modern ship. The exhaust stack of this ship offers four large nearly vertical surfaces on which a low profile antenna could be mounted. If the antennas offered near hemispherical coverage, two antennas mounted on opposite sides of the stack would provide total coverage.
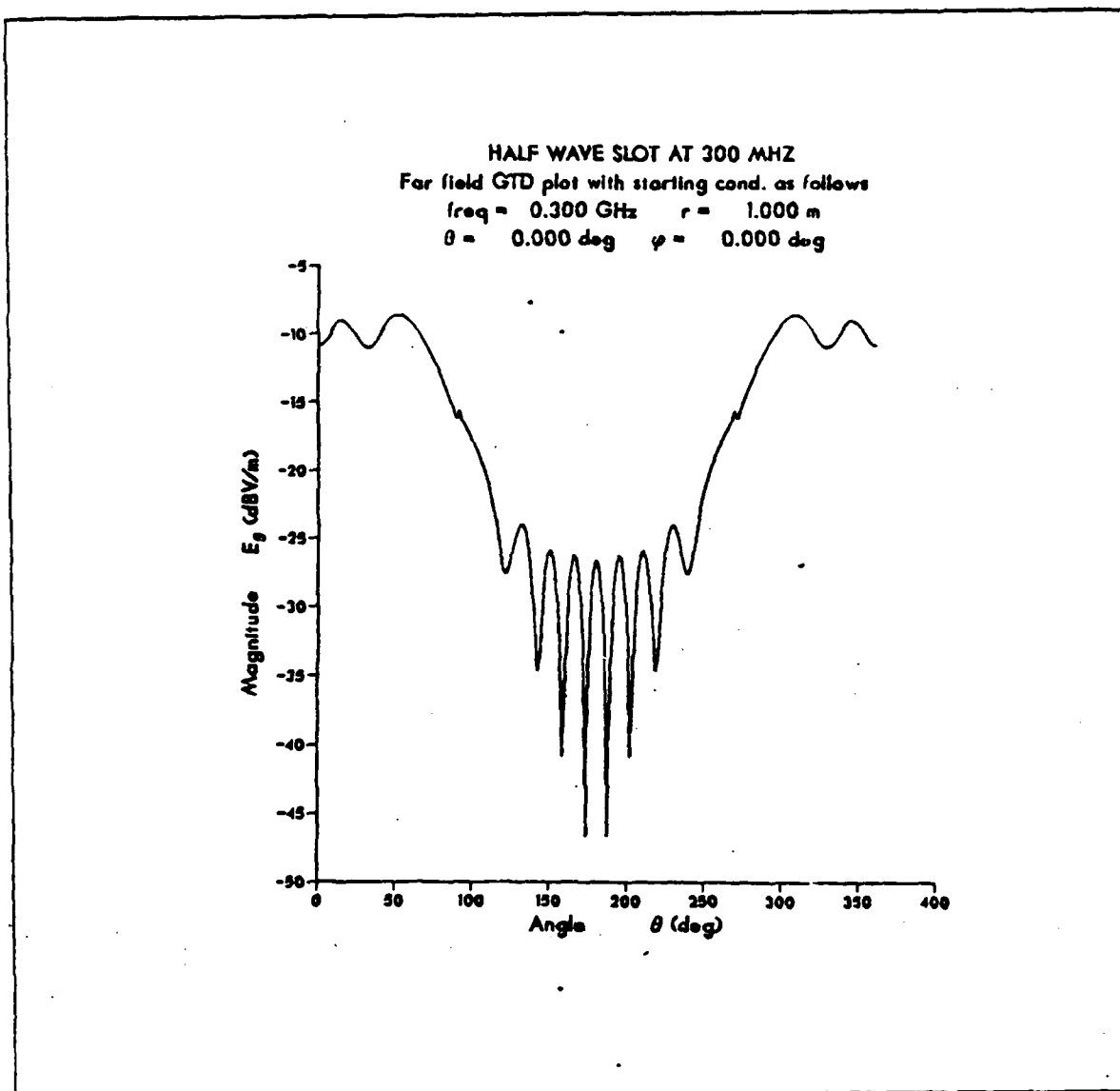
Figure 3.3   Radiation Pattern of Half Wavelength Slot, $\varphi = 0$, F = 300 MHz.

40
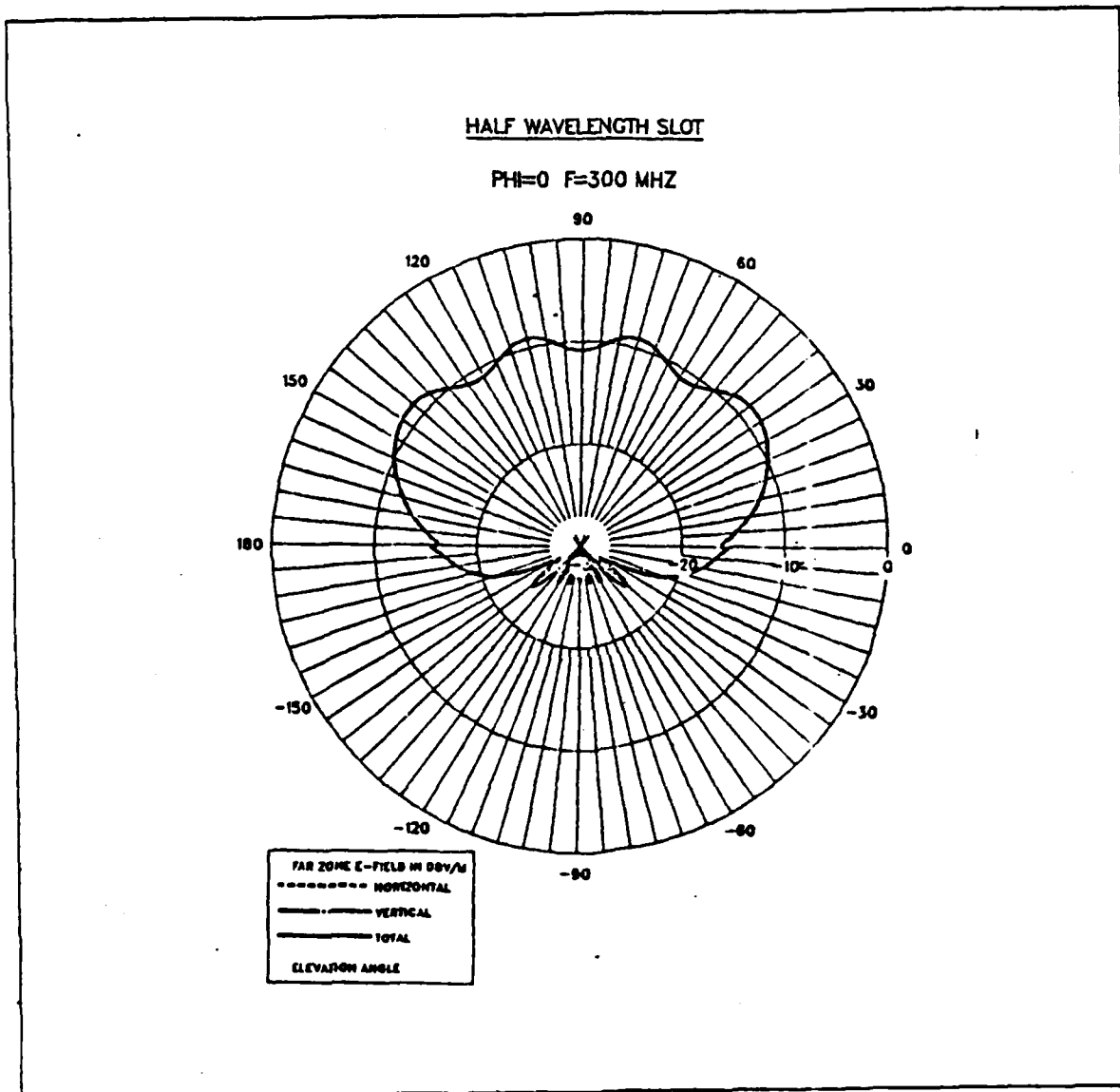
Figure 3.4   Radiation Pattern of Half Wavelength Slot, $\varphi = 0$, F = 300 MHz.

41

CROSSED SLOT AT 300 MHZ ON 4X4 METER PLATE
viewing point : φ = 0.00 deg
θ = 0.00 deg
r = 20.00 m

$\phi = 0$
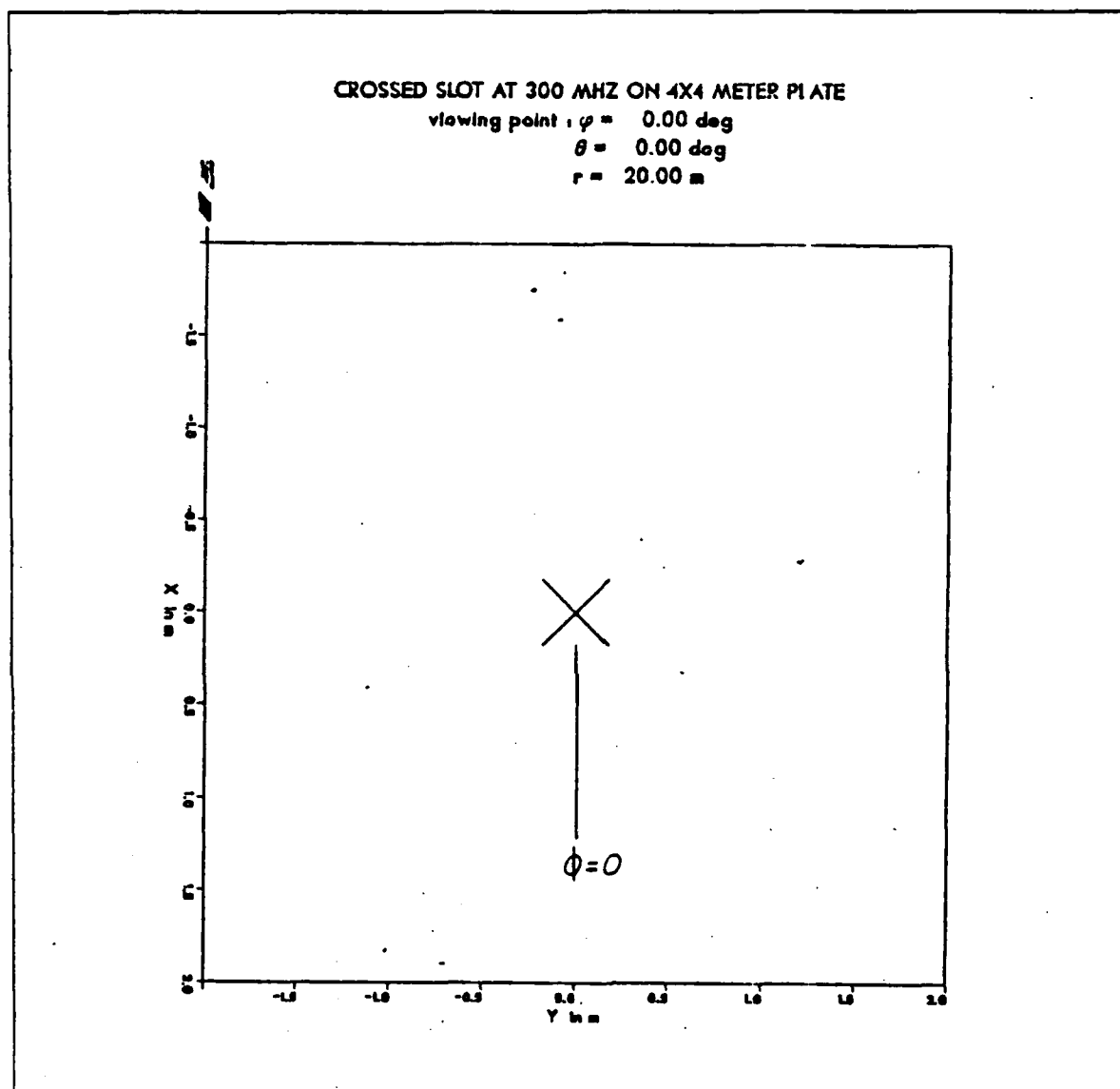
Figure 3.5   Half Wavelength Crossed-Slot at 300 MHz on 4x4 Meter Flat Plate.

42
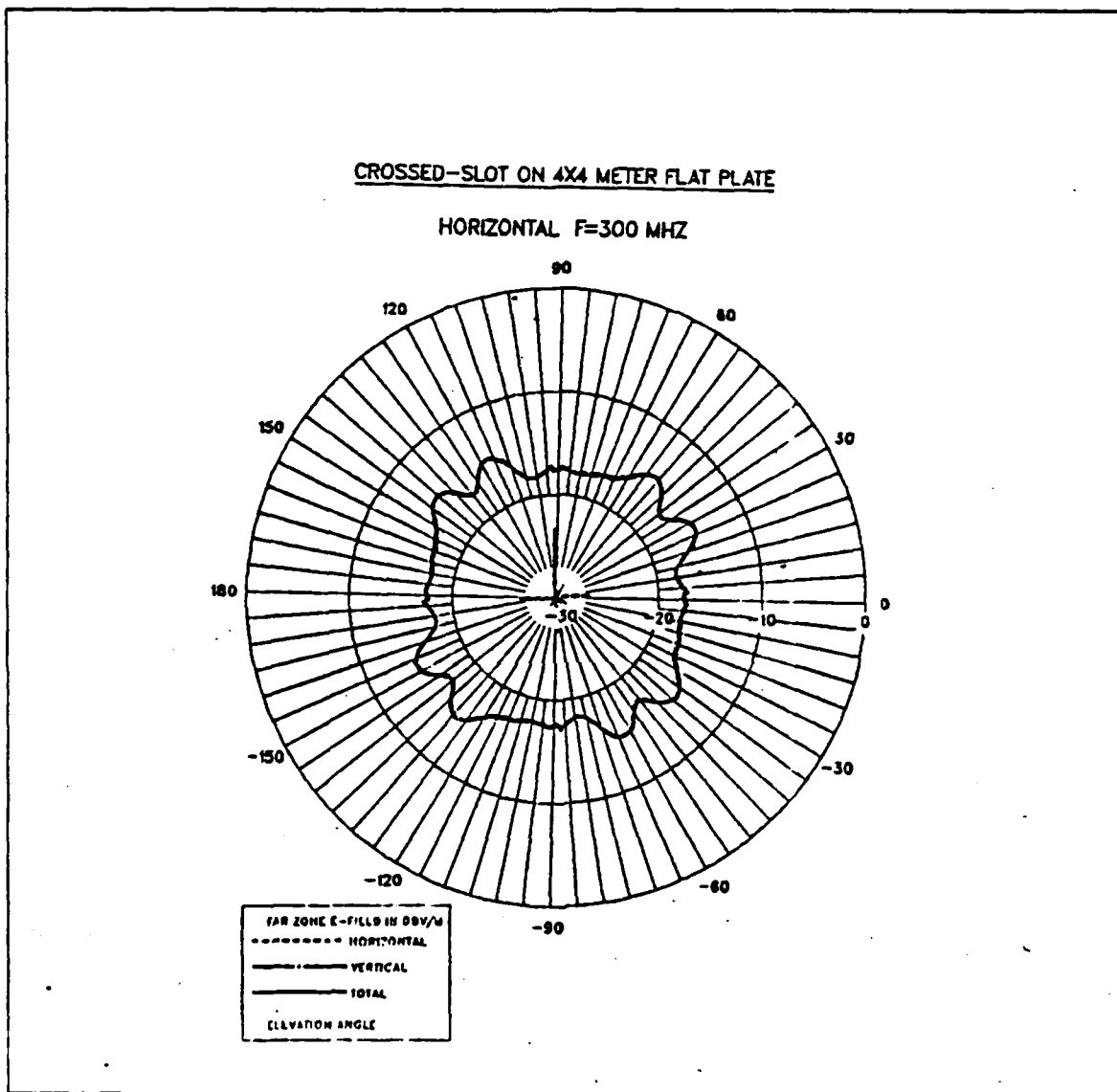
Figure 3.6   Horizontal Cut Radiation Pattern for Crossed-Slot Antenna, F = 300 MHz.
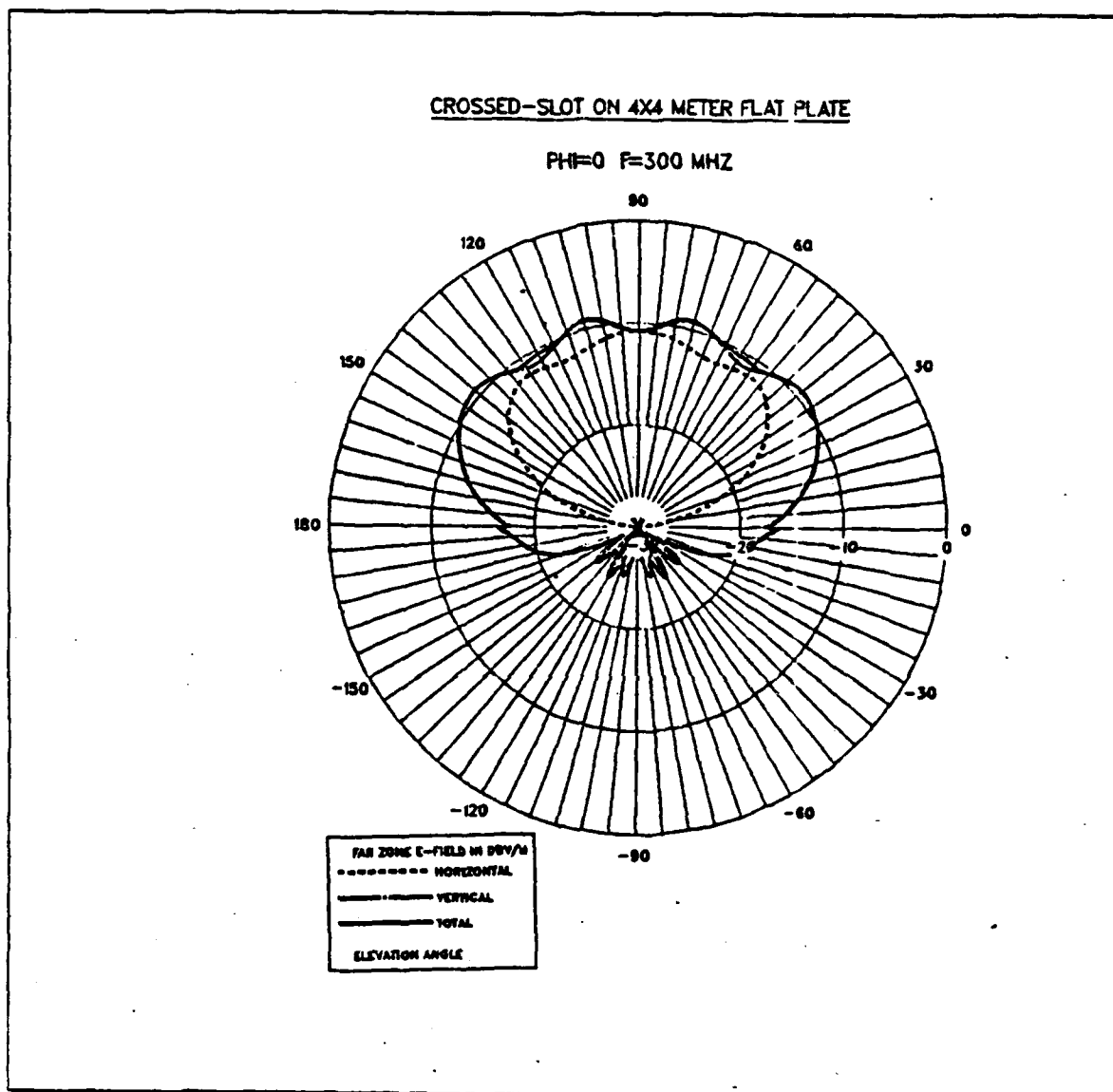
Figure 3.7   Vertical Cut Radiation Pattern for Crossed-Slot Antenna,
φ = 0, F = 300 MHz.

STARBOARD PROFILE

PLAN VIEW
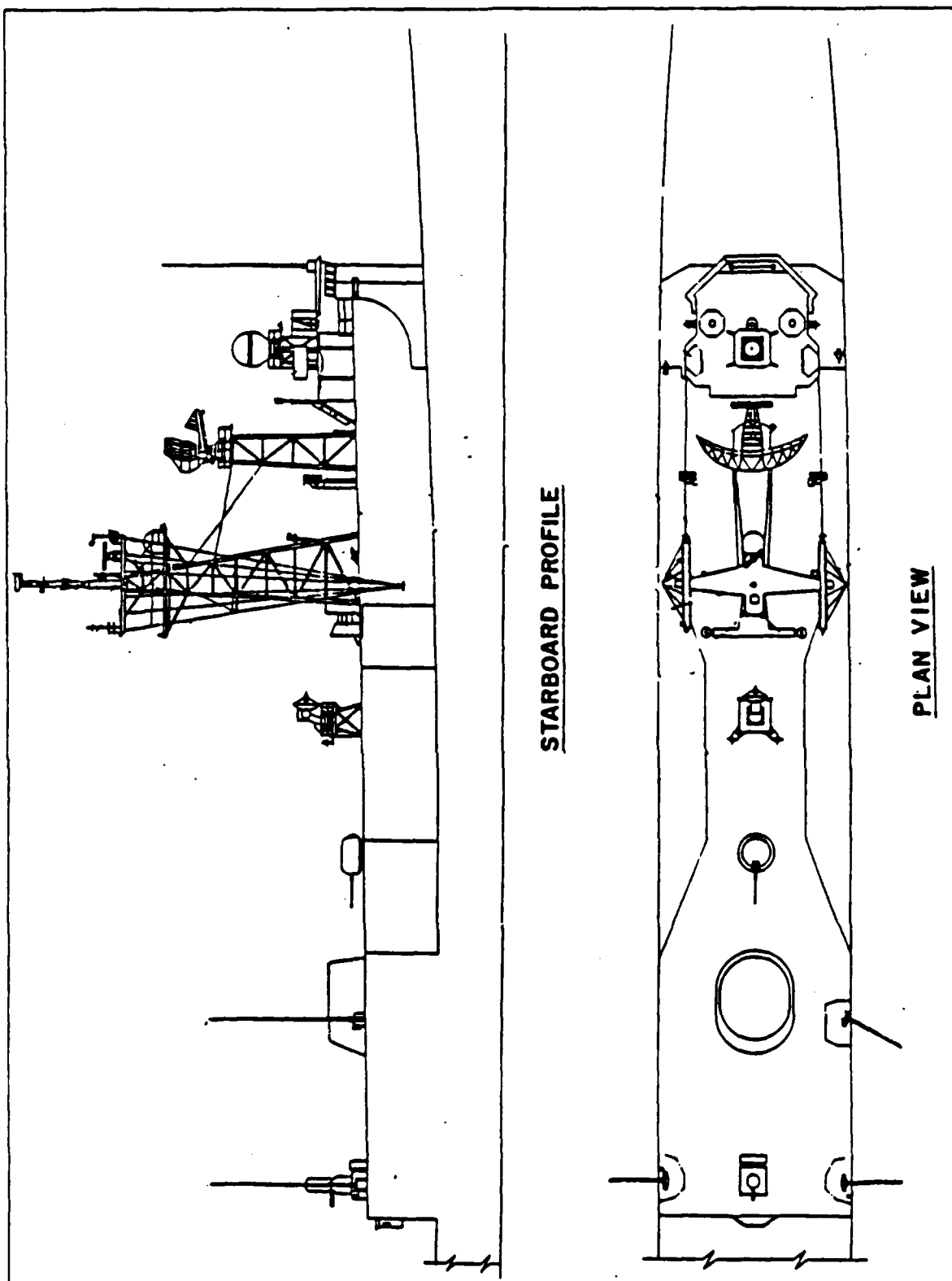
Figure 3.8   Partial Plan and Profile of Modern Frigate.

45

CROSSED SLOTS ON OPPOSITE SIDES OF STACK
viewing point : φ = 30.00 deg
θ = 60.00 deg
r = 50.00 m
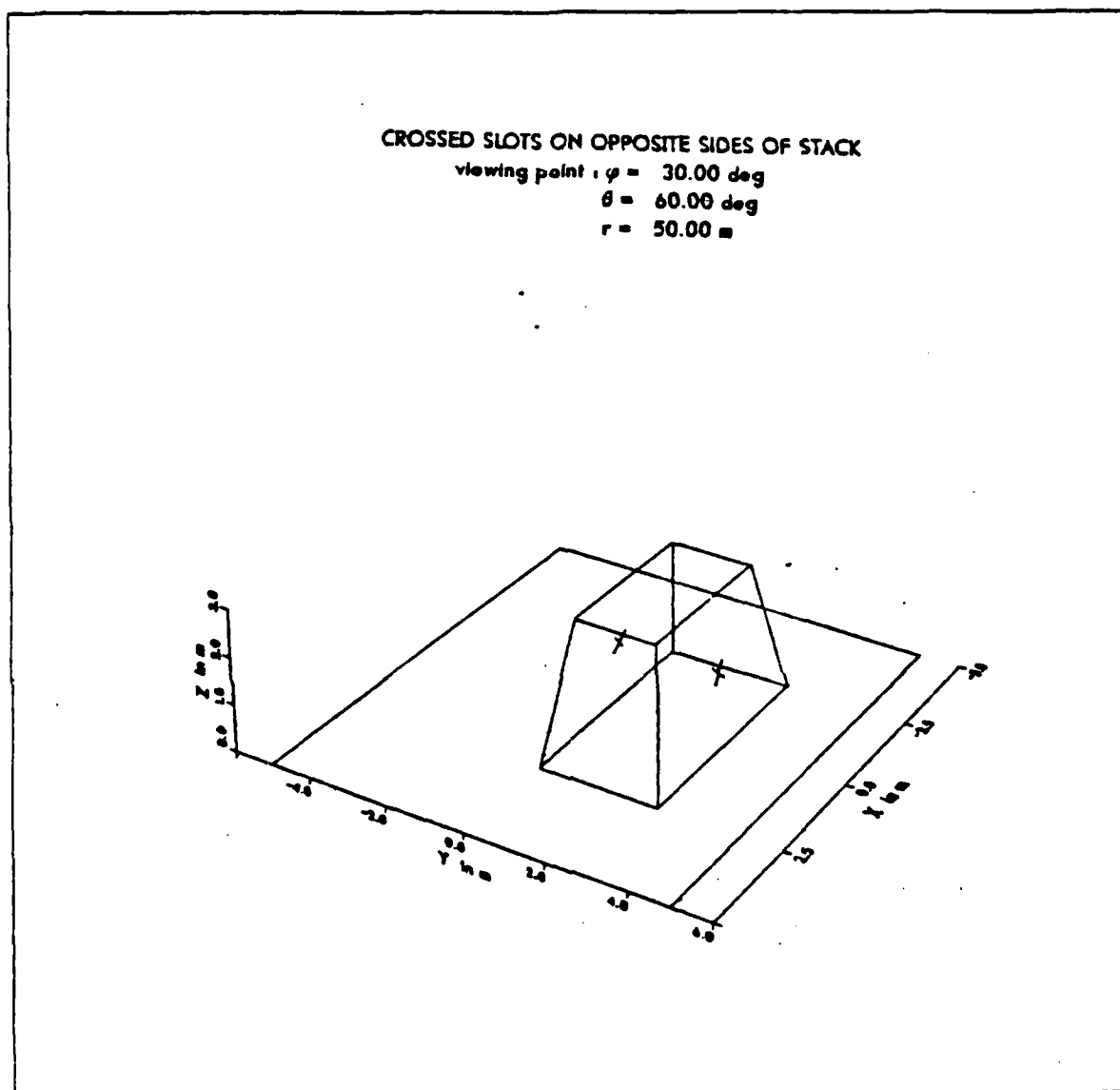
Figure 3.9   Simplified Model of Exhaust Stack With Crossed-Slot Antennas.

Figure 3.9 shows a simplified model for a ships exhaust with two crossed-slot antennas mounted on opposite sides. Figure 3.10 shows a view from overhead to show the orientation for the radiation patterns. Figures 3.11-3.13 show vertical pattern cuts
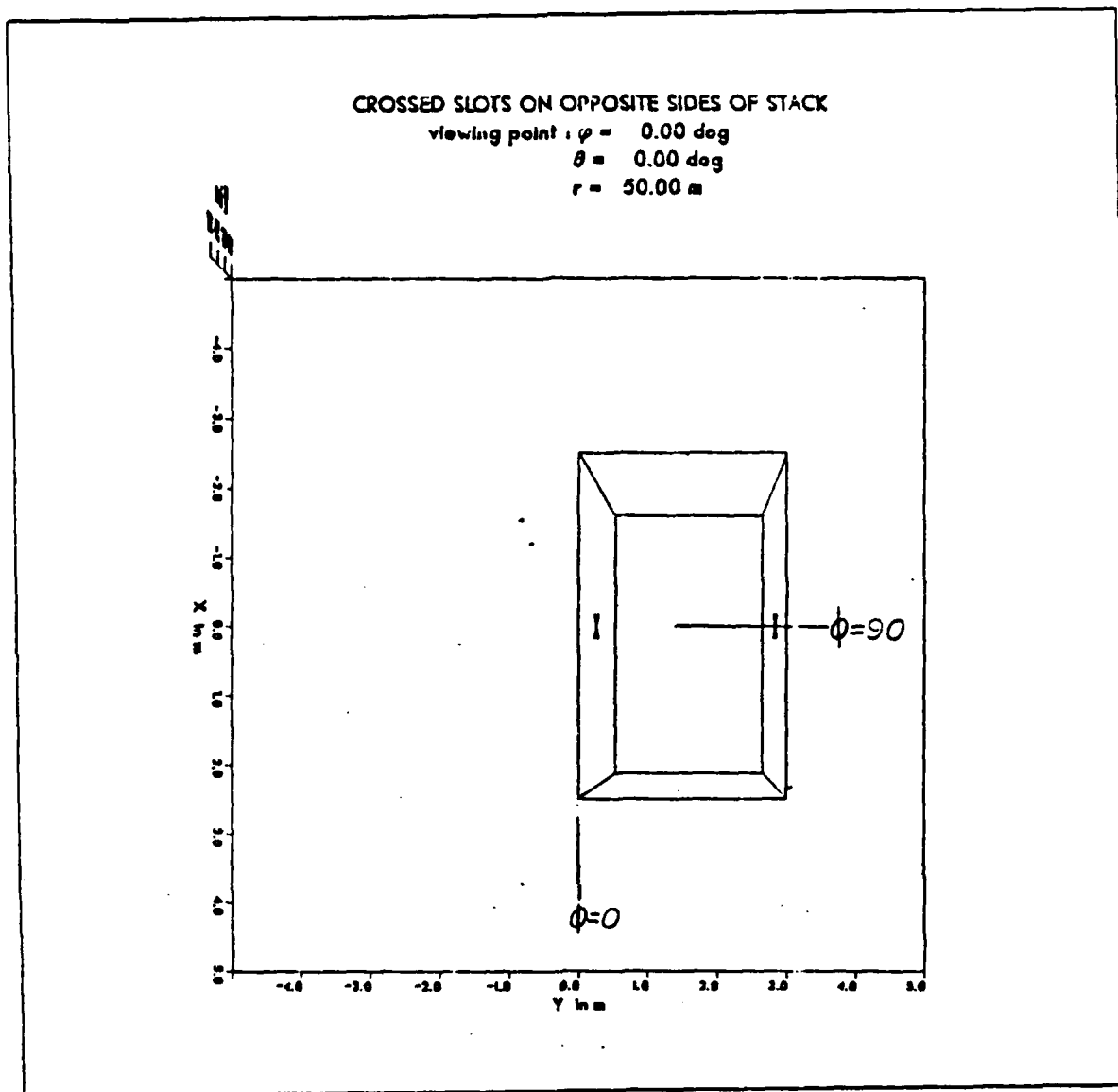
Figure 3.10 Overhead View of Exhaust Stack Showing Orientation of
Radiation Pattern Measurments.

for φ = 0,90 degrees and a horizontal cut above the stack. The null that appears at
165 degrees on Figure 3.11 which gives the pattern an unsymetrical appearance was
found to be caused by fields that are diffracted by the vertical plate edges then reflected
by the horizontal plate. From these patterns, one can see that this arrangement offers
nearly hemispherical coverage above the plane of the flat plate.

47
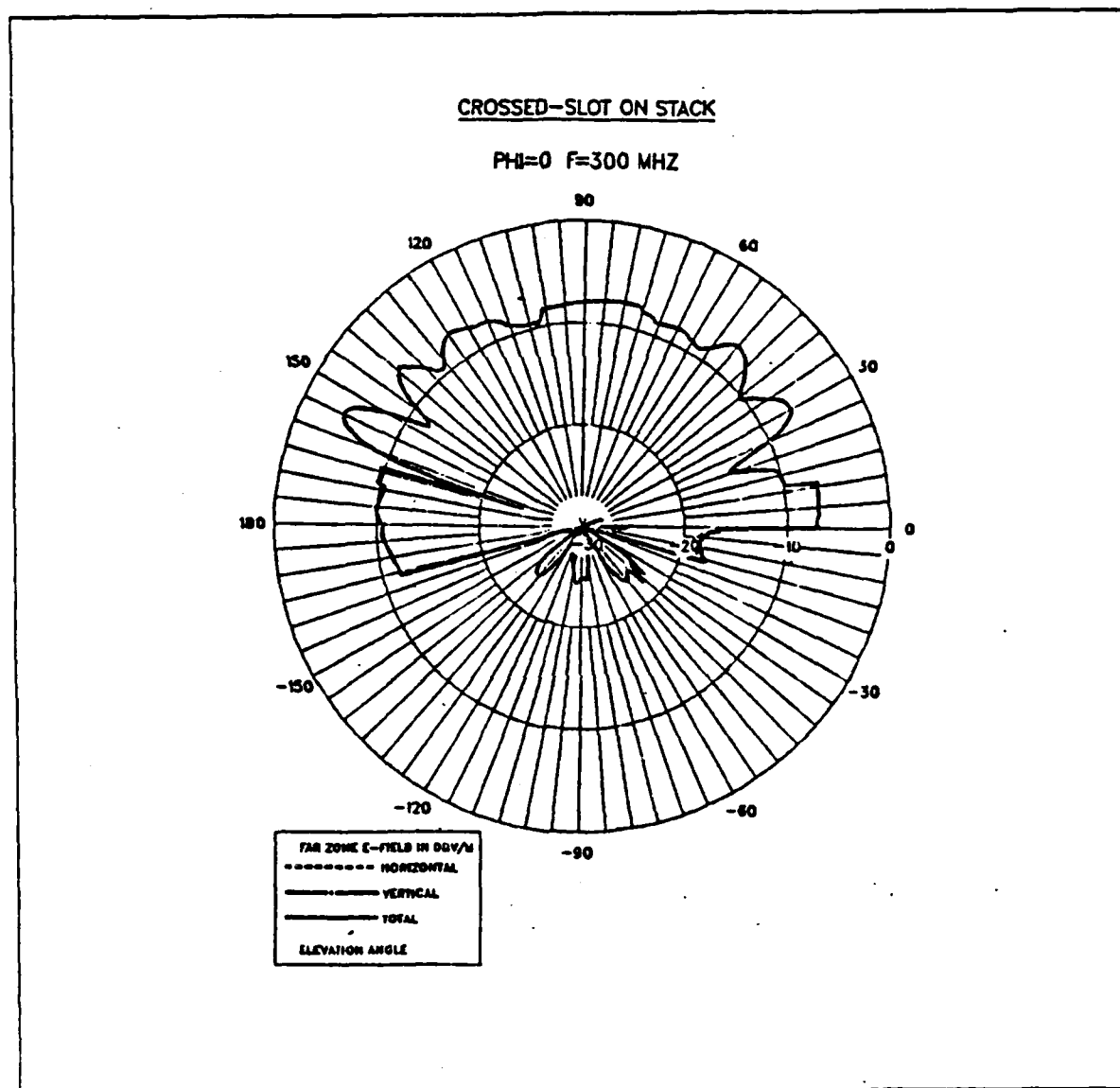
Figure 3.11   Radiation Pattern for Stack Mounted Crossed-Slots, φ = 0, F = 300 MHz.
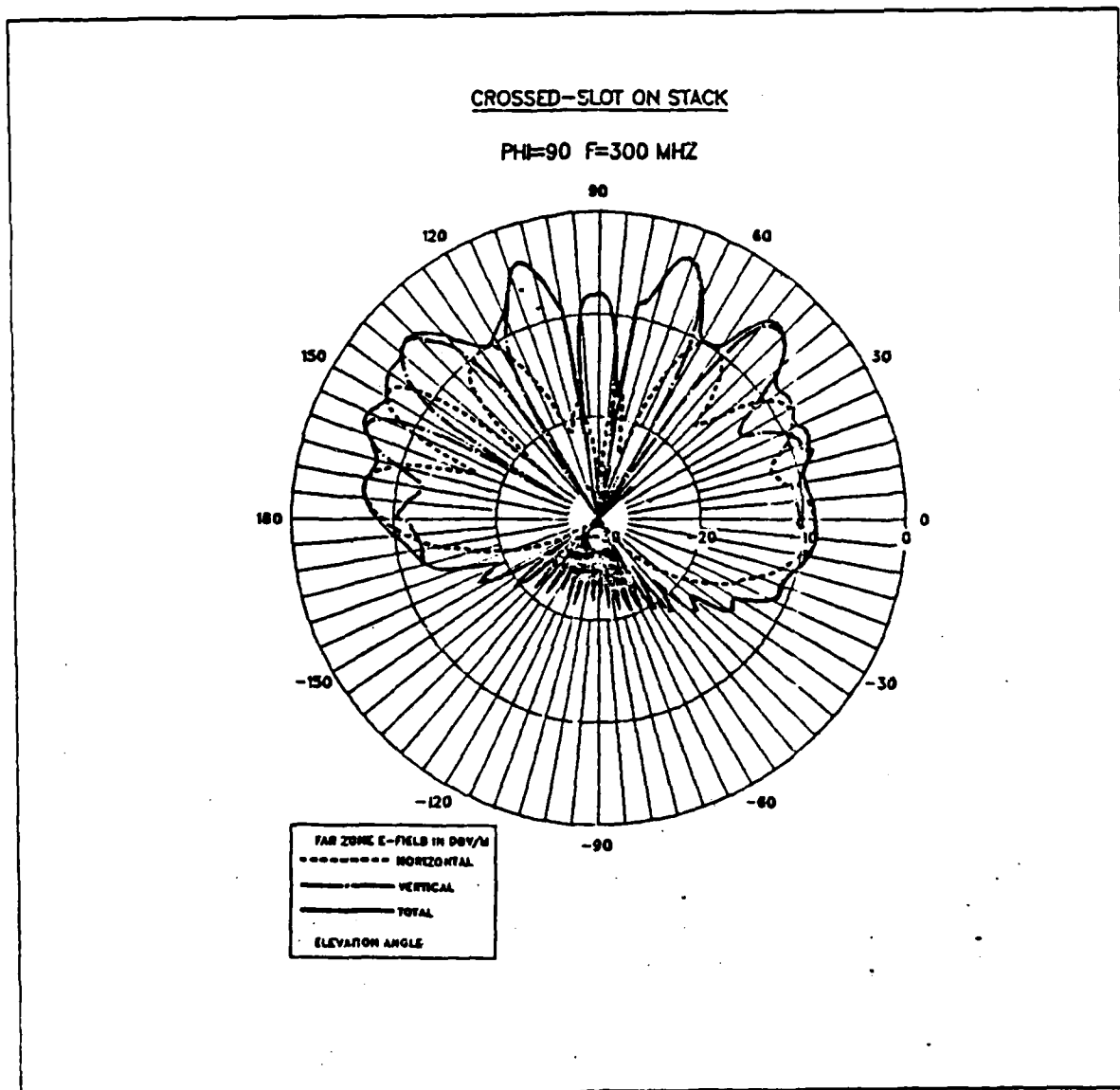
Figure 3.12   Radiation Pattern for Stack Mounted Crossed-Slots, $\varphi = 90$, F = 300 MHz.
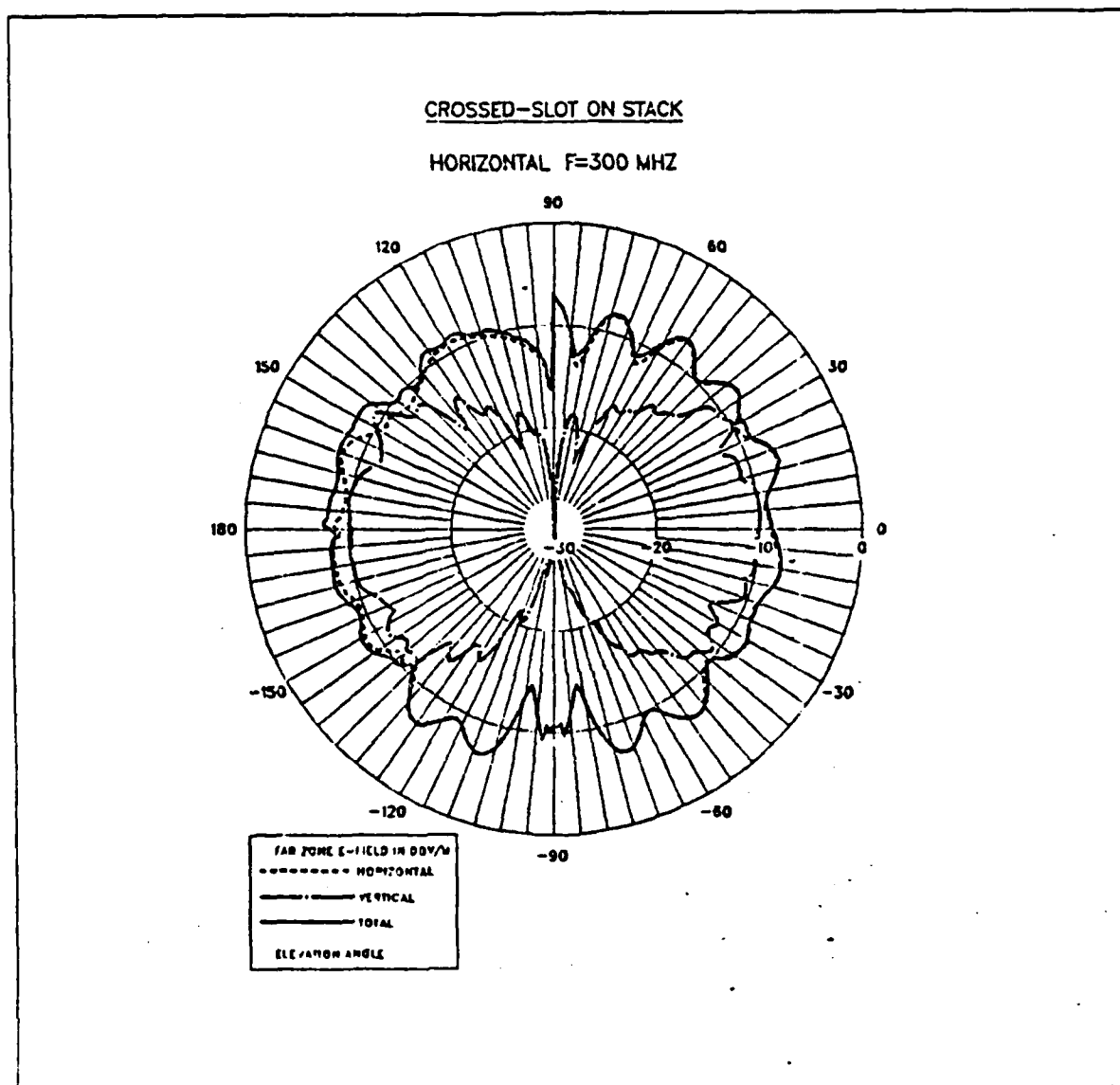
Figure 3.13   Radiation Pattern for Stack Mounted Crossed-Slots (Horizontal Cut),
F = 300 MHz.

IV. MONOPOLE-SLOT

A. PRINCIPLE OF OPERATION

One method of overcoming the problem of narrow bandwidth often associated with low profile antennas is the use of complementary elements such as the dipole and slot. The fields of these antennas are found to be related by Babinet's principle which gives the following relation between their impedances

$$Z_s Z_d = (60\pi)^2 \qquad \text{(eqn 4.1)}$$

where

Z_s = slot impedance, and

Z_d = dipole impedance.

If the slot and dipole impedances are normalized to 60π, Equation 4.1 becomes

$$Z_d = 1/Z_s = Y_s \qquad \text{(eqn 4.2)}$$

By properly combining these complementary elements, an antenna with relatively stable input impedance would result. [Ref. 3: p. 489]

The concept of utilizing complementary elements has been used several times in the past to produce combinational antennas. Itoh, Watanabe, and Matsumoto introduced a crossed-slot and monopole antenna for energy density reception [Ref. 13: pp. 485-489]. Wilkinson combined a small dipole in the plane of a slot to produce circular polarization [Ref. 14]. Mayes, Warren, and Weisenmeyer presented the monopole-slot antenna [Ref. 3: pp. 489-493] which was later improved and designated the hybrid slot [Ref. 15: pp. 1-7].

The principle of the monopole-slot is to combine the slot and monopole on the same feed line so their impedances, which have dual properties, can be utilized to produce a relatively stable input impedance independent of frequency. The monopole-slot is a two port transmission line network with the monopole representing a shunt load and the slot representing a series load. When one port of the network is

51
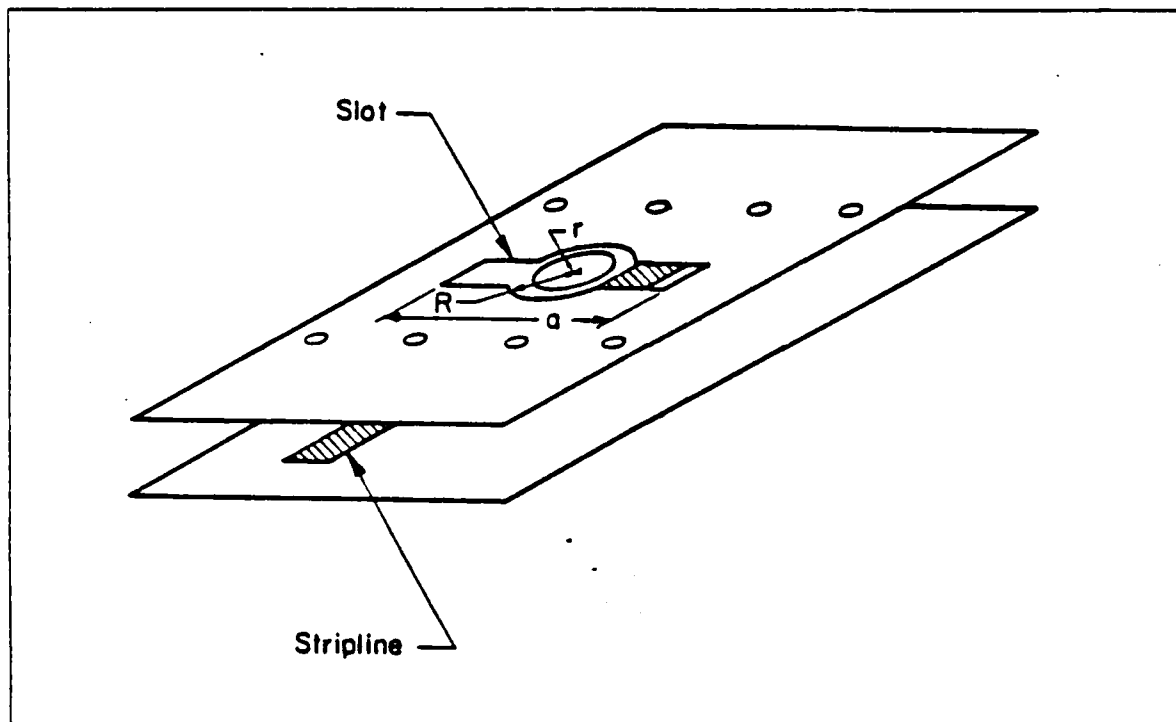
Figure 4.1   The Hybrid Slot Antenna (from Ref. 15).

terminated in the characteristic impedance of the transmission line, the resultant input impedance has less dependence on frequency than either of the elements acting independently.

The original monopole-slot shown in Figure 1.3 consisted of a cavity-backed slot combined with a monopole above the slot. This antenna is not in itself a low-profile antenna, but serves as a basis for developing the hybrid slot which is a low profile antenna.

In order to reduce the height of the monopole while maintaining the same resonant frequency, the monopole can be capacitively top-loaded with a circular disk. The height can be reduced with increased disk area until the circular disk is in the same plane with the slot as shown in Figure 4.1 Test results for a hybrid slot with R = 0.7 in, r = 0.65 in, and a = 5.2 in, reported by Mayes and Cwik indicate a VSWR of less than two over most of the band from 700 MHz to 1.36 GHz [Ref. 15: p. 2].

The radiation pattern of the hybrid slot is a combination of the patterns of the monopole and the slot. The horizontal pattern of the monopole is omnidirectional while the slot horizontal pattern is a figure eight (similar to the vertical pattern of a vertical dipole) with 180 degrees phase shift between the two lobes. If these patterns

52

are properly combined field addition occurs in one direction and cancellation occurs in the other, producing a cardioid. The direction of maximum radiation can be reversed by feeding the other port, causing cancellation in the opposite direction [Ref. 3: p. 492].

Attempts to model this antenna with NEC-MOM to demonstrate the wide impedance bandwidth have been unsuccessful primarily due to the sparse grid spacing required for the cavity (in order to maintain a reasonable number of segments). Although the impedance bandwidth is not demonstrated, the principle of operation can be demonstrated through radiation patterns as modeled by NEC-BSC.
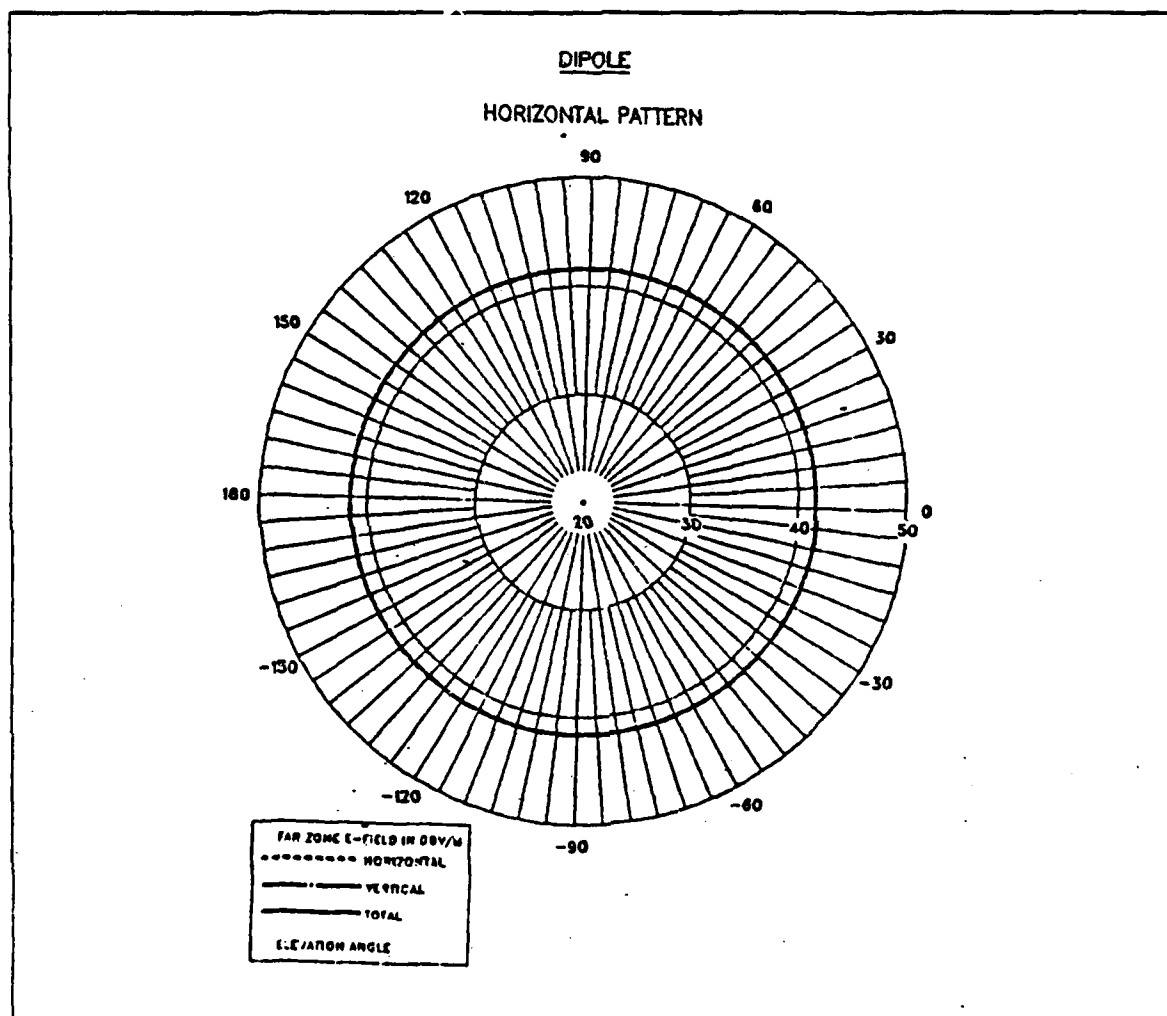
Figure 4.2   Horizontal Plane Pattern of Dipole.

Figure 4.2 and 4.3 show the horizontal plane patterns from a half wavelength dipole and a half wavelength slot modeled separately on a flat plate above a perfect

53
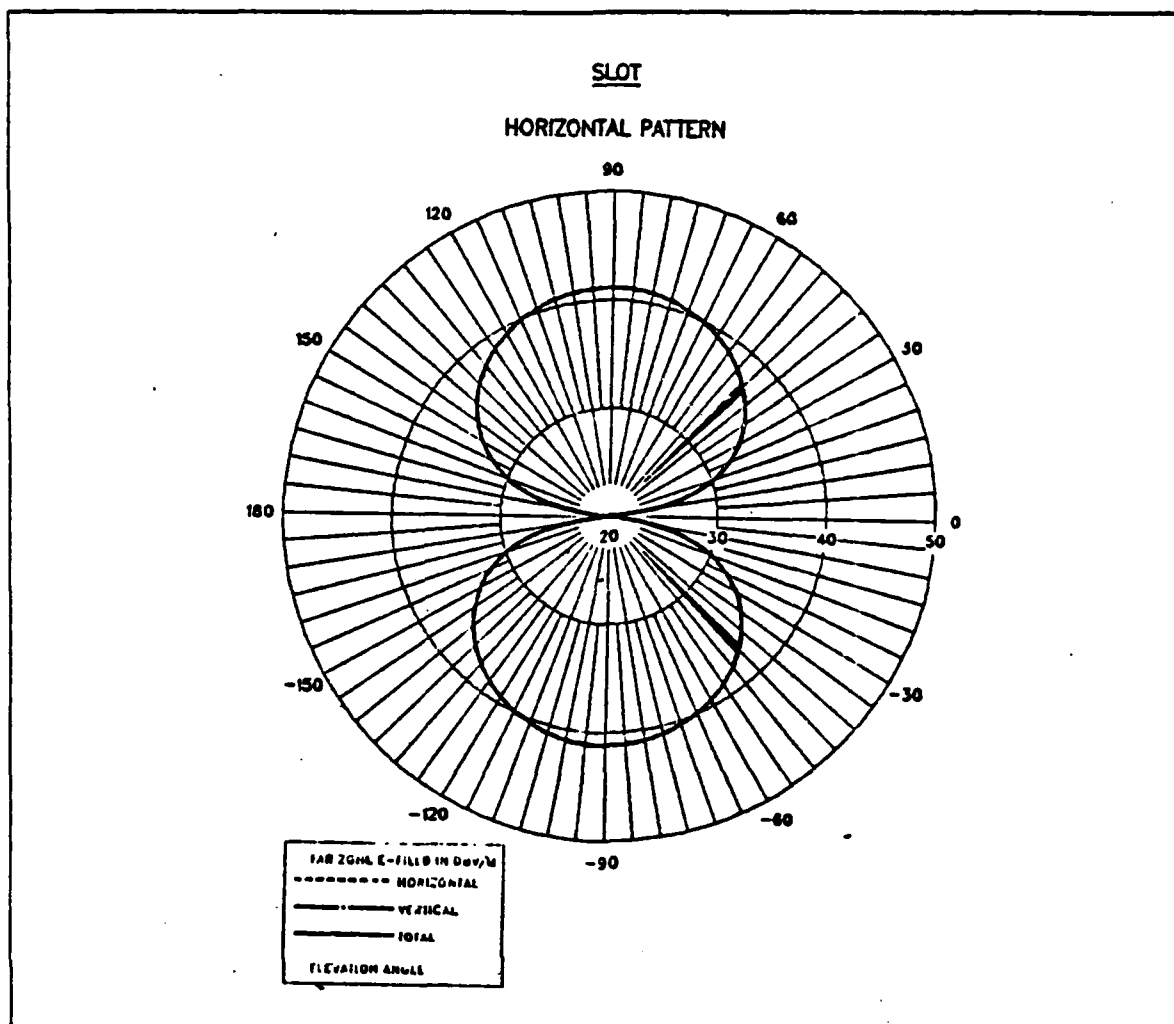
Figure 4.3   Horizontal Plane Pattern of Slot.

ground plane.. When the two are combined with the dipole directly above the slot, field cancellation and addition occurs and the pattern of Figure 4.4 results. Vertical cut patterns for $\varphi = 0$ and $\varphi = 90$ degrees are shown in Figures 4.5 and 4.6

Another property of an antenna of this type is its ability to reduce signal fading caused by standing waves since the monopole responds to electric field components and the slot responds to magnetic field components. [Ref. 13: p. 485]

54
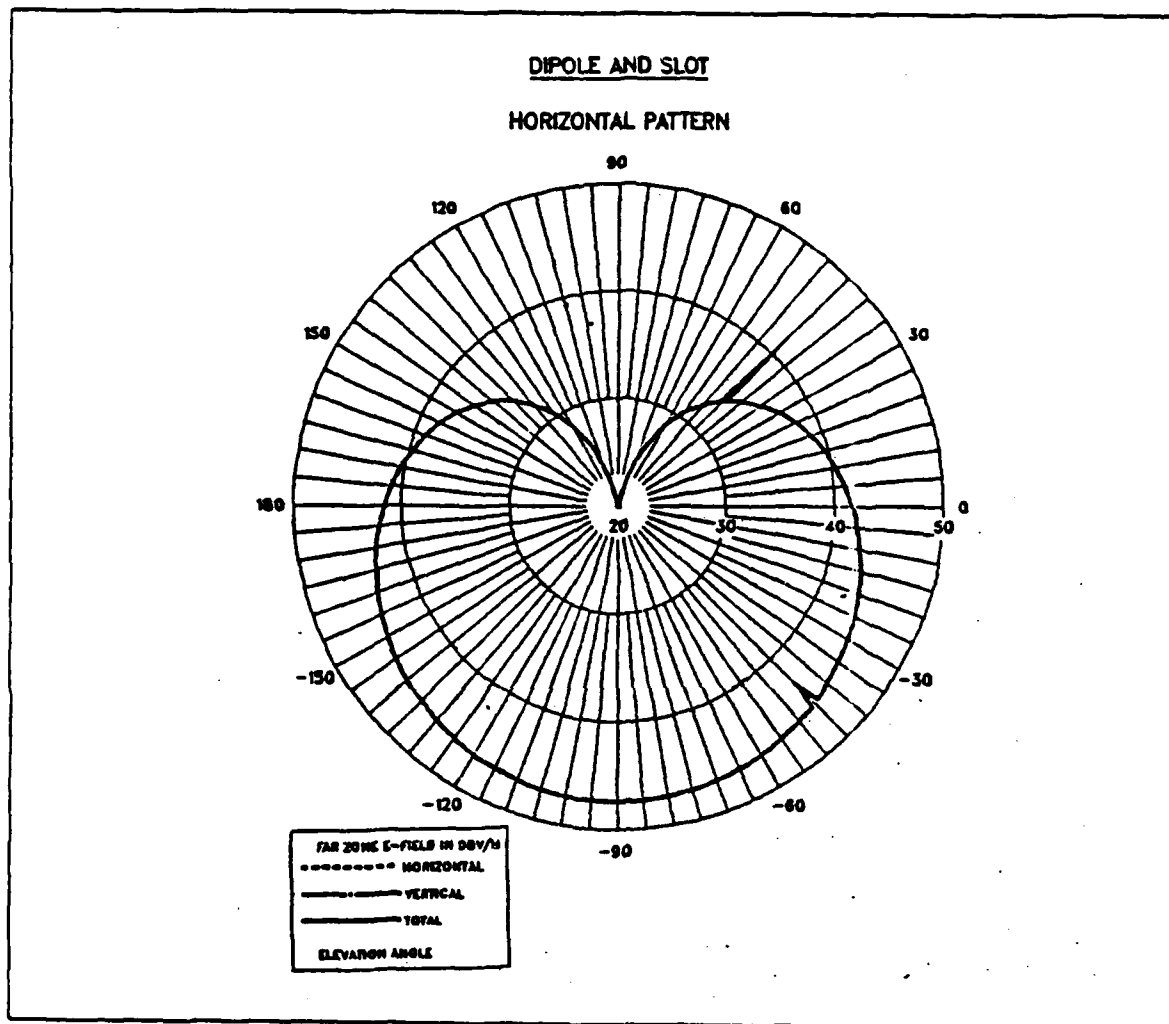
Figure 4.4   Horizontal Plane Pattern for Dipole and Slot.

55
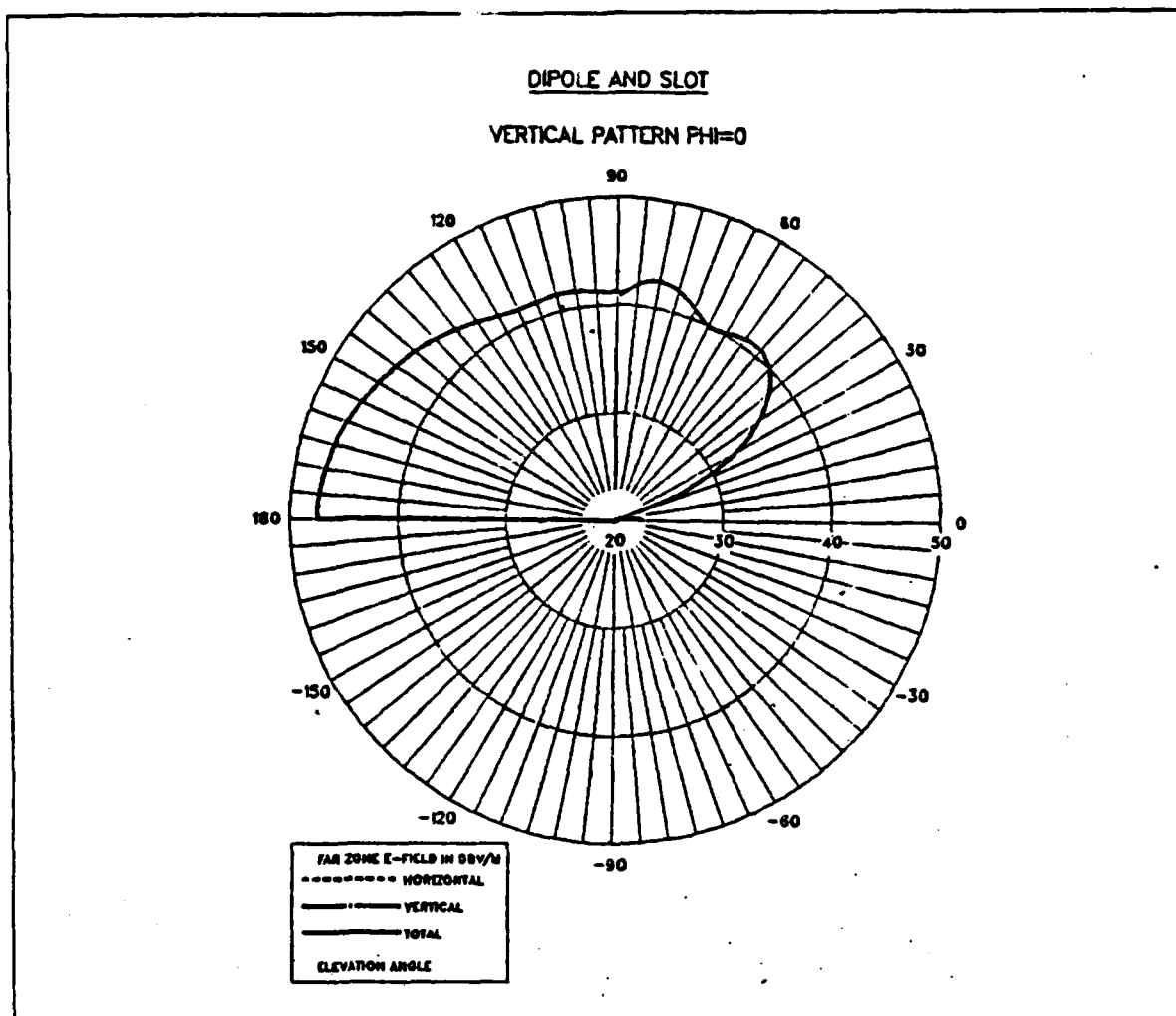
Figure 4.5   Vertical Plane Pattern for Dipole and Slot, $\varphi = 0$.
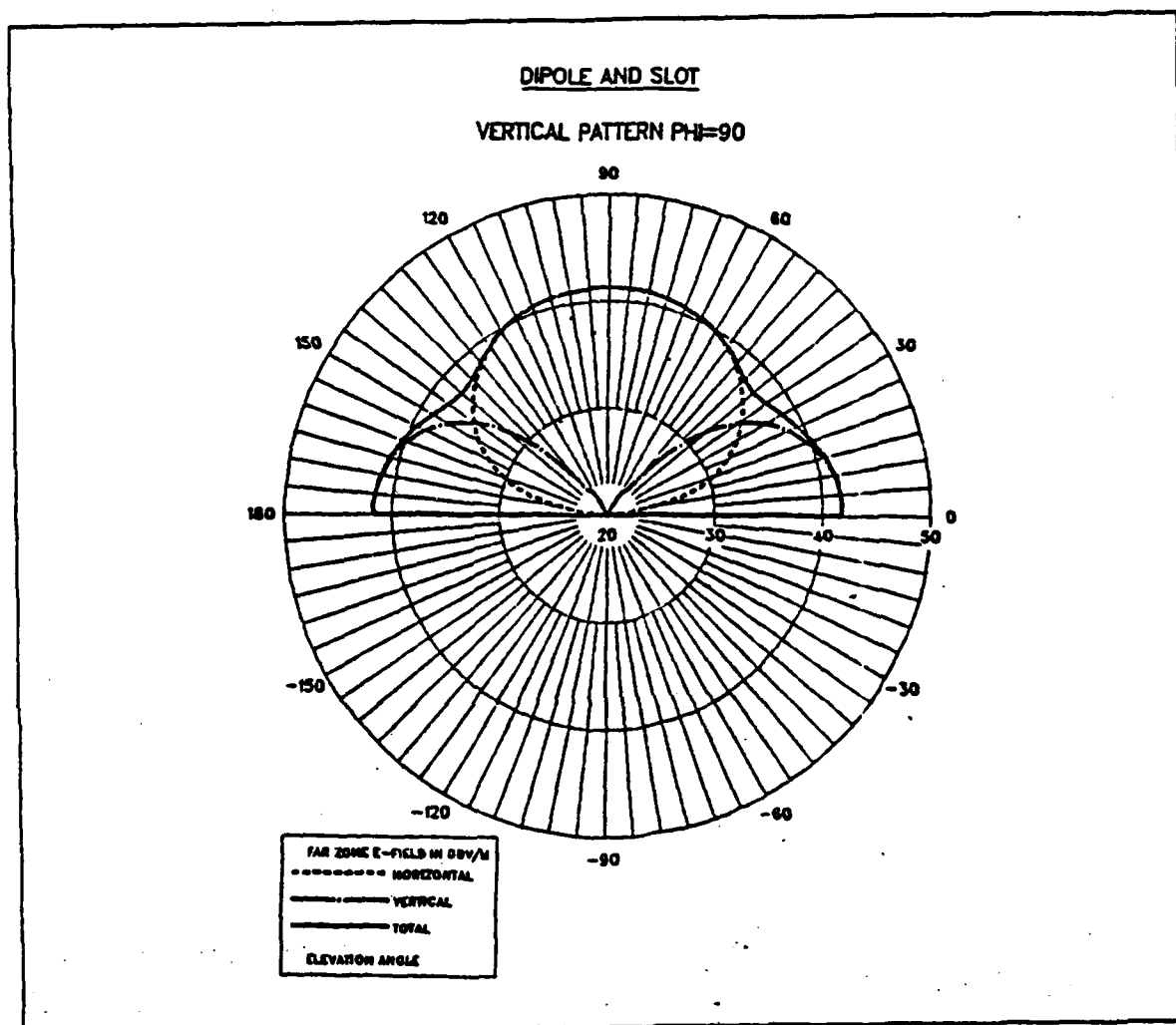
Figure 4.6   Vertical Plane Pattern for Dipole and Slot, $\varphi = 90$.

V. CONCLUSIONS AND RECOMMENDATIONS

A. CONCLUSIONS

Conformal antennas with excellent radiation properties have been available for some time, but disadvantages such as narrow bandwidth have kept them from replacing many present day antennas on ships. This work has demonstrated that there are methods available for increasing the bandwidth of these antennas without increasing complexity to a large degree.

In exploring these methods, the comparison of computer modeling results with experimental work indicates that the codes can be used to effectively reproduce real world antennas. This further indicates that the computer models can be used to predict characteristics of these antennas when subjected to further enhancement techniques.

B. RECOMMENDATIONS

The purpose of this work was to serve as an entry-level point in the investigation of VHF-UHF combat survivable antennas. While the three antennas chosen have shown potential, much more work is required before their operational deployment can be achieved.

The NEGCOMA model attempted to approximate experimental work already accomplished. The model should be further investigated to optimize the antenna with respect to resonator size and spacing, feedpoint location, and antenna height. Since the antenna is a microstrip, it could be easily constructed to determine other optimization factors such as dielectric type.

While the NEGCOMA exhibited a wider bandwidth than that of a single rectangular element, it is still a fairly narrow band antenna. In order to achieve an antenna with a bandwidth wide enough for practical use, the above optimization techniques should be applied to an antenna with four additional resonators.

The NEC-MOM is an excellent code for determining antenna characteristics, but cannot predict the antenna operation in a complex environment. To do this a source distribution could be developed from the MOM output for an antenna such as a NEGCOMA and used with the NEC-BSC to determine the operation in a real-world environment.

While experimental results for the ridged-cavity crossed-slot antenna are available, the antenna could possibly be further enhanced by utilizing different slot geometries such as a bow-tie or stepped slot. An accurate computer model for this antenna would be very complicated and would require considerable computing time. One possible recommendation would be to model the different slot geometries without the ridged cavity to compare their characteristics and build a scale model of the antenna.

The hybrid slot, although somewhat directional, has properties that warrant further investigation. In order to obtain hemispherical coverage while maintaining the wideband properties, two or more antennas could be used. The hybrid slot could also be constructed rather easily for actual experimentation.

LIST OF REFERENCES

1. Kumar, Girish and Kuldip C. Gupta, *Nonradiating Edges and Four Edges Gap-Coupled Multiple Resonator Broad-band Microstrip Antennas*, in *IEEE Transactions on Antennas and Propagation*, AP-33, no. 2, pp. 173-178, February, 1985

2. King, H.E. and J.L. Wong, *A Shallow Ridged-Cavity Crossed-Slot Antenna for the 240 to 400 MHz Frequency Range*, in *IEEE Transactions on Antennas and Propagation*, AP-23, no. 5, pp. 687-689, September, 1975

3. Mayes, Paul E. and others *The Monopole-Slot: A Small Broad-Band Unidirectional Antenna*, in *IEEE Transactions on Antennas and Propagation*, AP-20, no. 4, pp. 489-493, July, 1972

4. Jasik, Henry and Richard C. Johnson, *Antenna Engineering Handbook*, McGraw-Hill, New York, 1984

5. Carver, Keith R. and James W. Mink, *Microstrip Antenna Technology*, in *IEEE Transactions on Antennas and Propagation*, AP-29, no. 1, pp. 2-24, January, 1981

6. Blake, Lamont, *Antennas*, John Wiley and Sons, New York, 1966

7. Burke, G.J. and A.J. Pogio, *Numerical Electromagnetics Code-Method of Moments*, Naval Ocean Systems Center Technical Document 116, vol. 2, January, 1981

8. Booker, H.G., *Slot Aerials and Their Relation to Complementary Wire Aerials*, in *Journal of IEE(London)*, part IIIa, vol. 93, pp. 620-626, March, 1946

9. Milligan, Thomas A., *Modern Antenna Design*, McGraw-Hill, New York, 1985

10. Marhefka, R.J. and W.D. Burnside, *Numerical Electromagnetic Code-Basic Scattering Code, Part I: User's Manual, Version 2*, The Ohio State University Electroscience Laboratory Technical Report 7122 42-14 (713742), December, 1982

11. Koh, W.J., *Radiation Hazard Evaluation for a High Power Mobile Electromagnetic Radiation Weapon Using the Numerical Electromagnetic Code*, MSEE Thesis, Naval Postgraduate School, Monterey, California, March, 1987

12. Rudge, A.W. and others, *The Handbook of Antenna Design, Vol.II*, Peter Peregrinus Ltd, London, 1982

13. Itoh, Kiyohiko and others, *Slot-Monopole Antenna System for Energy-Density Reception at UHF* in *IEEE Transactions on Antennas and Propagation*, AP-27, no. 4, pp. 485-489, July, 1979

14. Wilkinson, E.J., *A Circularly Polarized Slot Antenna*, in *The Microwave Journal*, vol. 4, pp. 97-100, March, 1961

15. Mayes, P.E. and T. Cwik, *The Hybrid Slot*, in *Proceedings of Convergence 80, The 30th Annual Conference of the IEEE Vehicular Technology Society, International Conference on Transportation Electronics*, Dearborn, Michigan, pp. 1-7, September 15-17, 1980

INITIAL DISTRIBUTION LIST

No. Copies

1. Defense Technical Information Center   2
   Cameron Station
   Alexandria, VA 22304-6145

2. Library, Code 0142   2
   Naval Postgraduate School
   Monterey, CA 93943-5002

3. Department Chairman, Code 62   1
   Department of Electical and Computer Engineering
   Naval Postgraduate School
   Monterey, CA 93943-5000

4. Harold Askins   1
   NESEC Charleston
   4600 Goer Rd.
   N. Charleston, SC 29406

5. W.P. Averill, CAPT.   1
   U.S. Naval Academy
   Department of Electrical Engineering
   Annapolis, MD 21402

6. R. Raschke, GE Elec. Co. BLDG 3, RM 3312   1
   P.O.Box 2500
   Daytona Beach, FL 32015

7. J.J. Reaves JR., Naval Elec. Sys. Eng. Cntr.   1
   4600 Marriott Dr.
   N. Charleston, SC 29413

8. Alfred Resnick, Capital Cities Comm. ABC Radio   1
   1345 Ave. of Americas 26th Floor
   New York, NY 10105

9. John W. Rockway, NOSC Code 822(T)   1
   271 Catalina Blvd.
   San Diego, CA 92151

10. E. Thowless, NOSC Code 822(T)   1
    271 Catalina Blvd.
    San Diego, CA 92151

11. W.F. Flanigan, NOSC Code 825   1
    271 Catalina Blvd
    San Diego, CA 92152

12. M. Selkellick, Code 825   1
    David Taylor Naval Ship Research
    Development Center
    Bethesda, MD 20084-5000

13. Robert Latorre   1
    Lawrence Liv. Nat'l. Lab.
    P.O. Box 5504, L-156
    Livermore, CA 94550

14. Dr.Tom Tice   1
    Department of Electrical and Computer Engrg.
    Arizona State University
    Tempe, AZ 85287

15 Dr. Roger C. Rudduck   1
    Ohio State University
    Electrophysics Laboratory
    1320 Kinnear Rd.
    Columbus, OH 43212

16. Commander Naval Space and   1
    Naval Warfare Systems Command
    Attention: Dick Pride
    PDW 110-243
    Washington D.C. 20363

17. Naval Sea Systems Command   1
    Attention: P. Law
    C61X41
    Washington, D.C. 20362

18. James Tertocha   1
    C-15 Tenbytowne Apts.
    Delran, NJ 08075

19. LT Dimitris Koutsouras, H.N.   1
    250 Forest Ridge, #72
    Monterey, CA 93940

20. LT George Lymberopoulos, H.N.   1
    Ferron St. 48-50
    Athens 104.40, GREECE

21. Director Research Administration, Code 012   1
    Naval Postgraduate School
    Monterey, CA 93943-5000

22. Moray King   1
    Evring Research Institute
    1455 W 820 N
    Provo, UT 84601

23. H. Kobavashi   1
     1607 Cliff Dr.
     Edgewater, MD 21037

24. LT Kevin Purvis   2
     P.O. Box 475
     Jesup, GA 31545

25. Donald Wehner NOSC Code 744   1
     Naval Ocean Systems Center
     San Diego, CA 92152

26. R.W. Adler   5
     Naval Postgraduate School, Code 62AB
     Monterey, CA 93943-5000

27. Dan Baran   1
     IITRI
     185 Admiral Cochrane Dr.
     Annapolis, MD 21401

28. J.K. Breakall   1
     Lawrence Liv. Nat'l. Lab.
     P.O. Box 5504, L-156
     Livermore, CA 94550

29. Brenton Campbell   1
     ILL Inst. Of Technology
     Annapolis, MD 21401

30. Al Christman   1
     Ohio University
     Stocker Center
     Athens, OH 45701

31. Dawson Coblin   1
     Lockheed M & S Co.
     0/6242;B/130/ Box 3504
     Sunnyvale, CA 94088-3504

32. Dave Faust   1
     Eyring Research Inst.
     1455 W 820 N
     Provo, UT 84601

33. Dr. A.J. Ferraro   1
     Penn. State Univ.
     Ionosphere Res. Lab.
     University Park, PA 16802

34. Dr. S.J. Kubina   1
     Concordia University
     7141 Sherbrooke St. West
     Montreal, QUE H4B1R6

35. Mr. Jim Logan   1
   NOSC Code 822(T)
   271 Catalina Blvd.
   San Diego, CA 92152

36. R.J. Marhefka   1
   Ohio State University
   1320 Kinnear Road
   Columbus, OH 43212

37. Janet McDonald   1
   Commander, USAISEIC/ASBI-STS
   Ft. Huachuca, AZ 85613-7300

38. E.K. Miller   1
   Rockwell Science Center
   Box 1085
   Thousand Oaks, CA 91365

39. I.C. Olson   1
   NOSC Code 822(T)
   271 Catalina Blvd.
   San Diego, CA 92152

40. H.A. Atwater   1
   Naval Postgraduate School, Code 62AN
   Monterey, CA 93943-5000

END
Feb.
1988
DTIC

END

Feb.

1988

DTIC